MCR-86-2601
NAS8-36108

Volume X

Aerocapture for Manned Mars Missions

Orbital Transfer Vehicle Concept Definition and System Analysis Study

1987

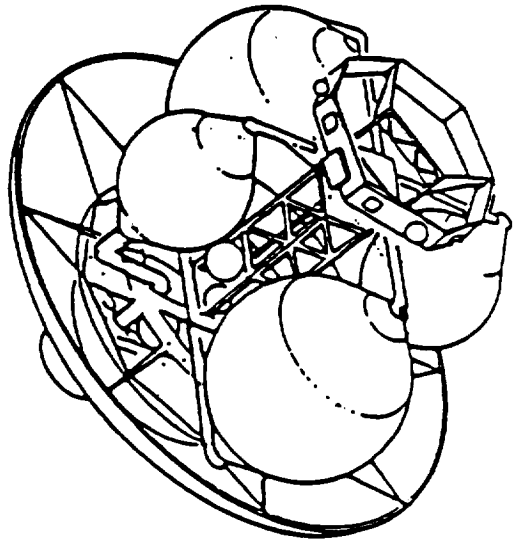

MARTIN MARIETTA

OTV

MCR-86-2601
NAS8-36108

ORBITAL TRANSFER VEHICLE
CONCEPT DEFINITION AND SYSTEM ANALYSIS STUDY

VOLUME X

AEROCAPTURE FOR MANNED MARS MISSIONS

January 1987
Rev 1 - Jan 1988

Prepared By: _____
W. H. Willcockson
OTV Program Manager

Approved By: _____
Glen J. Dickman
Advanced Upper Stages

MARTIN MARIETTA
ASTRONAUTICS GROUP
P.O. BOX 179
DENVER, COLORADO 80201

(5

This final report, Volume X - Aerocapture for Manned Mars Missions, was prepared by Martin Marietta Astronautics Group for NASA/MSFC in accordance with contract NAS8-36108. The study extension was conducted under the direction of NASA OTV Study Manager, Mr. Donald R. Saxton, during the period from June 1986 to January 1987.

The following personnel were key contributors during this study extension:

Study Manager:	W. H. Willcockson
Denver Engineering Support:	
Aerothermal	G. W. Heckel
Flight Analysis Support	C. M. Reed
Michoud Engineering Support:	
Engineering Manager	W. P. Haese
Structural Analysis	R. B. Newton

This report supplements the OTV Phase A Study program results which were presented in Volumes I through IX.

Volume	Contents
Volume I	Executive Summary
Volume IA	Executive Summary Supplement
Volume II	OTV Concept Definition and Evaluation
	Book 1 Mission and System Requirements
	Book 2 OTV Concept Definition
	Book 3 Subsystem Trade Studies
	Book 4 Operations
Volume III	System and Program Trades
Volume IV	Space Station Accommodations
Volume V	Work Breakdown Structure and Dictionary
Volume VI	Cost Estimates
Volume VII	Integrated Technology Development Plan
Volume VIII	Environmental Analyses
Volume IX	Study Extension I Results
Volume X	Aerocapture for Manned Mars Missions

TABLE OF CONTENTS

VOLUME X - AEROCAPTURE FOR MANNED MARS MISSIONS

LIST OF TABLES AND FIGURES

ACRONYMS

ANARS	Autonomous Navigation and Attitude Reference System
AU	Astronomical Unit
FSI	Flexible Surface Insulation
GPS	Global Positioning System
L/D	Lift/Drag
MEM	Mars Excursion Module
OTV	Orbital Transfer Vehicle
RSI	Rigid Surface Insulation
VLBI	Very Long Base Interferometry

1.0 Introduction

A manned expedition to Mars has been under consideration as a potential mission for the early 21st century (Ref. 1). The necessarily large vehicle requirements have sparked interest in aerocapture as a means of reducing propellant usage. This volume summarizes the work performed to establish concepts and feasibility of such a mission which makes maximum use of aeroassist maneuvers.

2.0 Vehicle Baseline Description

The baseline vehicle for this study is shown in Figure 2.0-1 which is taken from Reference 1. The spacecraft can accommodate 6 people on a 2 year round trip voyage to Mars. It consists of three major sections: A Mars excursion module (MEM), a Laboratory and Habitation (Lab/Hab) module, and a Mars escape stage. The Mars excursion module is used to land on the planet

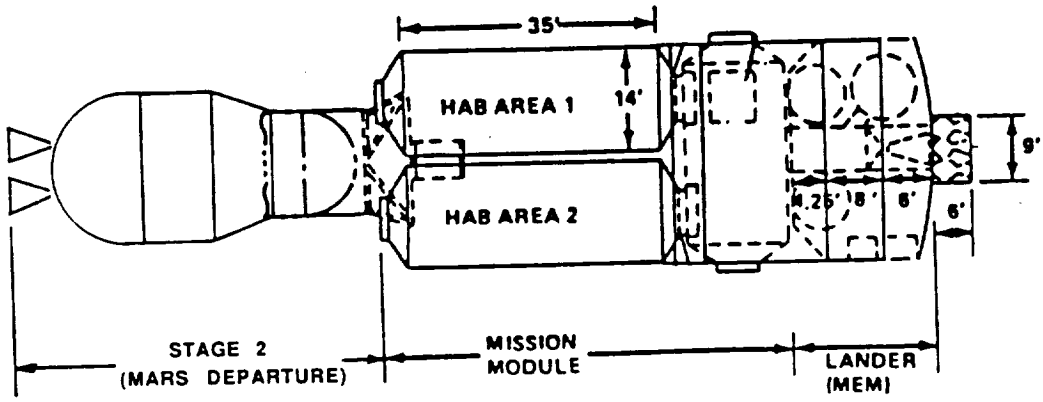

Figure 2.0-1 - Baseline Mars Vehicle Configuration

and perform surface investigations. The lower section serves as a launch platform for the MEM stage 2 which returns the crew and expedition samples to Martian orbit. The Lab/Hab module, which contains the living quarters and experiment laboratories, acts as a base vehicle in Mars park orbit while the MEM is on the surface. The Mars escape stage provides the impulse for departure from Martian orbit as well as any other correction maneuvers in the mission. The baseline weights for these modules is summarized in Table 2.0-1.

Table 2.0-1 - Baseline Vehicle Weights

	DRY WEIGHT (LB)	WET WEIGHT (LB)
MARS EXCURSION MODULE	74532	157527
LAB / HAB MODULES	100903	133676
MARS ESCAPE STAGE	15547	174056

3.0 Environmental Data

Mars and Earth planetary data are summarized in Table 3.0-1. The Mars base atmosphere is the Northern summer nominal as contained in the Mars Reference Atmosphere by A. Kliore, et al (Reference 2). Earth Nominal atmosphere is the 1962 standard.

Table 3.0-1 - Planetary Data

	EARTH	MARS
EQUATORIAL RADIUS	2.09256627E7 FT	1.114567E7 FT
POLAR RADIUS	208555024E7 FT	1.107448E7 FT
SPIN RATE	7.292115146E-5 RAD/SEC	7.0882181E-5 RADIAN/SEC
GRAVITY CONSTANT (MU)	1.407645794E16 FT3/SEC2	1.512468E15 FT3/SEC2
GRAVITY: J2 TERM	0.0010826	0.001965
GRAVITY: J3 TERM	-0.000002565	0
GRAVITY: J4 TERM	-0.000001608	0
ATMOSPHERE (NOMINAL)	1962 STANDARD	NORTH SUMMER NOMINAL (MARS REFERENCE ATMOS.)

4.0 Mission Profiles

The round-trip manned Mars mission has three major aerobraking phases. Upon arrival at Mars from the Earth an aeromaneuver is performed in the Martian atmosphere which reduces velocity to within elliptical orbit speeds. This is the Mars capture phase. Once the Mars vehicle has achieved a stable orbit about the planet, the MEM landing craft is deployed. Aerobraking is utilized to provide the majority of velocity reduction required to reach the surface of the planet. This is the Mars landing phase. After completing its surface mission, the Mars lander is propulsively boosted back into Martian orbit where it rejoins the Lab/Hab modules. After a period of on-orbit checkout and Mars/Earth phasing, the resulting stack is propulsively boosted into a trans-Earth trajectory. Upon arrival at Earth, another aerocapture maneuver is used to brake the vehicle into an elliptical Earth parking orbit. This last maneuver is the Earth capture phase.

An overview of the aerocapture process is shown in Figure 4.0-1. Beginning with a hyperbolic encounter trajectory the vehicle makes a grazing pass through the planet's atmosphere near orbital perigee. The amount of drag produced in this entry is controlled to yield a precise velocity reduction consistent with the targeted capture orbit at atmospheric exit. This capture orbit is highly eccentric to achieve synchronism with the planet. The perigee of this orbit is subsequently raised out of the atmosphere via a burn at the first pass through apogee. This results in a stable park orbit which is relatively free of further drag effects.

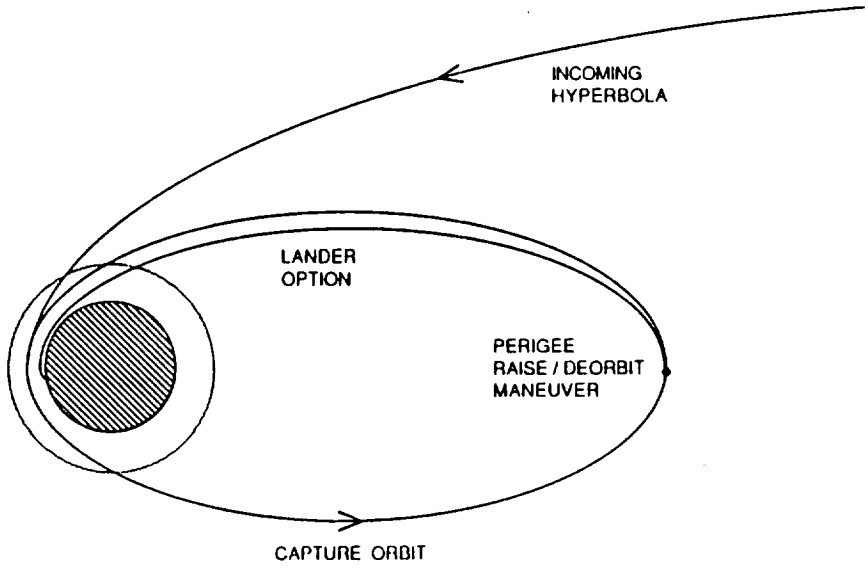

Figure 4.0-1 - Planetary Aerocapture

4.1 Mars Capture

The Mars vehicle encounters the planet on a hyperbolic (escape) trajectory and must be slowed to within planetary capture velocity. The completion of this phase results in the vehicle achieving a closed eccentric orbit about the planet. The Mars encounter hyperbolic selected for this study has a characteristic C_3 of 31 km^2/sec^2 representing an opposition class mission. The post-aerocapture orbit is Mars-synchronous with an apogee of 18108 nmi. and a period of 24.6 hr.

During the final days of pre-encounter a closed loop astronavigation process continuously refines the Mars encounter orbit. This process will probably use an autonomous device, such as the ANARS (Autonomous Navigation and Attitude Reference System) space sextant, to minimize vehicle/crew impacts. The results of this navigation refinement process will be utilized in a discrete number of terminal correction burns to increase the precision of the Mars entry state. The final trajectory correction is conducted at entry minus one hour. OTV experience has shown that a final correction burn at this time is operationally feasible and results in great benefits to aeroassist efficiency by reducing L/D requirements. The actual aerocapture maneuver lasts only about 4 minutes during which time active control of the vehicle exit conditions (apogee and orbit plane) is accomplished by controlled pointing of the aerodynamic lift vector. After exiting the atmosphere the vehicle is reconfigured for orbital operations. Upon reaching the apoapsis of its park orbit some 12 hrs after aerocapture, a perigee raise burn is executed which injects the vehicle into its operational Martian park orbit of 250 x 18108 nmi. This burn has a nominal value of 80 fps.

4.2 Mars Landing

The Mars landing phase is initiated when the Mars excursion module (MEM) separates from the Lab/Hab Orbiter stack and performs an 81 fps deorbit maneuver at the 18108 nmi. apogee point. This burn targets perigee at the proper altitude within the Martian atmosphere to produce a nominal aeroentry profile. During the orbital down-leg segment, astronavigation is conducted to refine the expected entry state. A terminal correction burn is performed an hour before entry. During the aerodynamic entry phase, lift is used to null downrange and crossrange errors to the landing site. After the aerodynamic phase is complete, descent rockets will be utilized to land on the surface of the planet. Following a period of exploration, rocket propulsion is utilized to boost the MEM Stage 2 back into Martian orbit for rendezvous with the waiting Lab/Hab stack.

4.3 Earth Capture

An aerocapture maneuver is utilized at Earth return to place the Mars vehicle in a closed Earth orbit. This maneuver maximizes the vehicle's efficiency since the same aerobrake hardware used for Mars capture can be reused for Earth capture. However, the issue of contamination of the Earth in the case of a failed aeromaneuver must be addressed in future studies for their impact on the overall practicality of this maneuver.

The same encounter strategy used for Mars capture is employed, with terminal astronavigation being utilized to correct the encounter trajectory. An additional advantage for this encounter is the use of the Earth-based GPS (Global Positioning System) signals in the final hours before entry to derive an extremely accurate state vector. As before, a terminal correction burn is conducted an hour before entry.

The Earth encounter hyperbola selected for the study has a characteristic C_3 of 68 km^2/sec^2 which represents a worst-case opposition class mission. This high energy encounter is the major driver in sizing the Mars/Earth capture brake as will be seen later. The post-aerocapture orbit is an eccentric Earth synchronous type with an apogee of 38484 nmi. and a perigee of 245 nmi. Injection into this orbit is accomplished at first apogee after the aeropass via a 78 fps burn. Subsequent to achieving this park orbit an earth-based OTV or a second aeropass (velocity reduction of 8890 fps) can retrieve the Mars craft back to a low Earth orbit. An alternate approach would be to retrieve only the crew and expedition samples, thus leaving the Mars craft in a high energy Earth orbit in preparation for another trip.

5.0 Entry Parametrics

Computer simulations of lifting entries were utilized to generate a data base for all three mission phases: Mars capture, Mars landing, and Earth capture. The mission profiles described in Section 4 were used to define desired entry and exit conditions.

5.1 Mars Capture Parametrics

Various entry trajectories were generated utilizing a pre-entry hyperbola with a C_3 of 31 km^2/sec^2 and a Mars capture apogee of 18108 nmi. (post-aero). Aerodynamic L/D and ballistic coefficient were varied for continuous lift up and lift down trajectories to generate the parametric data base. This data is displayed in Figures 5.1-1 and 5.1-2. Because of natural sensitivities the data on pre-entry perigee altitude and peak deceleration (Figure 5.1-1) is shown as a function of L/D while the peak heating and integrated heating (Figure 5.1-2) is shown as a function of ballistic coefficient.

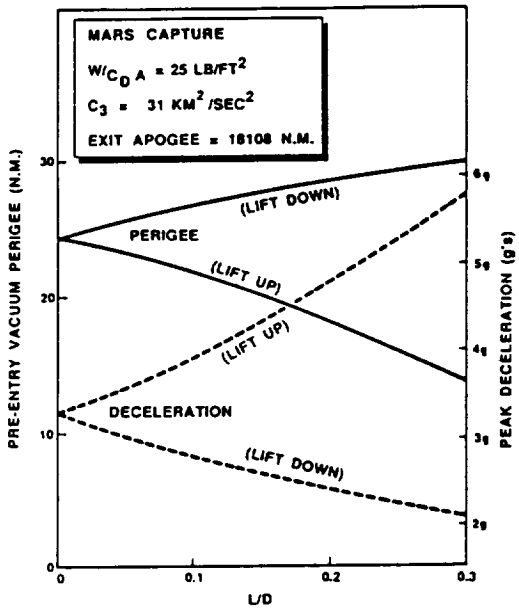

Figure 5.1-1 -
Mars Capture - L/D Parametrics

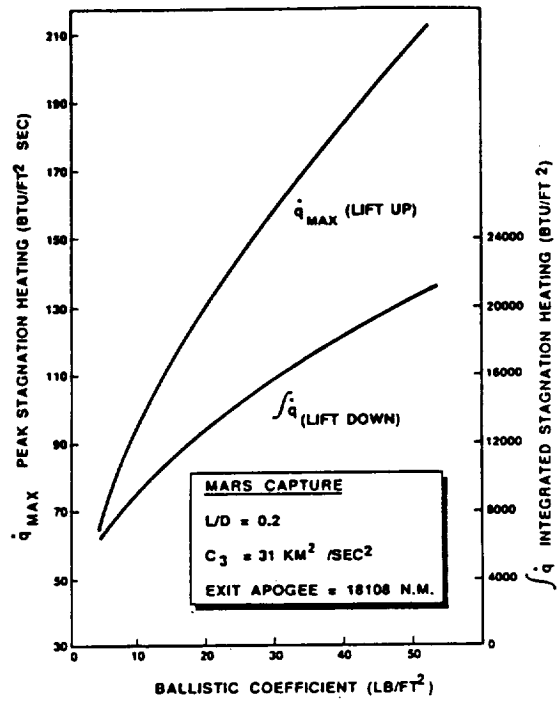

Figure 5.1-2 -
Mars Capture - Heating Parametrics

The difference between the pre-entry vacuum perigees for lift up and lift down aerotrajectories defines a control corridor width which represents the region in which the vehicle can be controlled to the desired exit conditions with the available lift (Figure 5.1-1). Once error analysis (Section 6) defines the magnitude of this control corridor, the vehicle's required L/D is set. From a width of 0.0 nmi. for a no lift condition the control corridor grows to a width of 16.0 nmi. at an L/D of 0.30.

Peak entry deceleration is shown in g's for lift up and lift down trajectories. The highest values of deceleration are always encountered in the continuous lift up case which is thus used as a worst case loading condition for structural sizing.

Peak stagnation heating shown in Figure 5.1-2 determines which TPS materials are acceptable for the aerobrake. The lift up condition shown generates maximal peak heating values. Integrated stagnation heating is shown for the lift down maximal condition. This parameter determines the required thickness of the aerobrake's insulating TPS.

Time histories of key parameters for the lift up and lift down Mars capture entries are shown in Appendix A and B.

5.2 Mars Landing Parametrics

A diagram of the landing entry process is shown in Figure 5.2-1. Trajectories were generated which had the proper pre-entry apogee as well as post-entry landing location ($\beta_{landing}$) for continous lift up and lift down entries. By varying ballistic coefficient and L/D a parametric data base was generated as shown in Figures 5.2-2 and 5.2-3. Orbital apogee at entry interface is 18108 nmi. and the landing point location is 8^{o} downrange of the pre-entry perigee location. This downrange parameter, $\beta_{landing}$, was sized to give load relief to the vehicle during entry while also avoiding skipout limits.

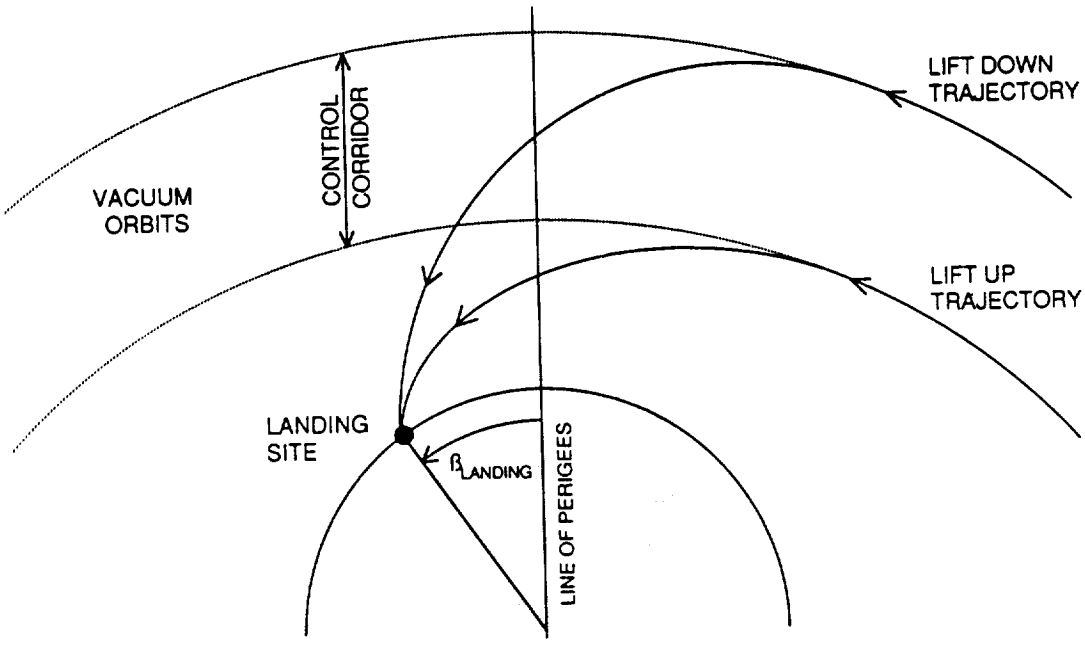

Figure 5.2-1 - Mars Landing Overview

Figure 5.2-2 shows pre-entry vacuum perigee and peak entry deceleration as a function of L/D. As is shown in Figure 5.2-1, an entry control corridor can be defined from the perigee differences of the lift up and lift down extremums. This control corridor width reaches a value of 12.1 nmi. for a 0.15 L/D. The peak deceleration levels are much lower than those associated with Mars capture.

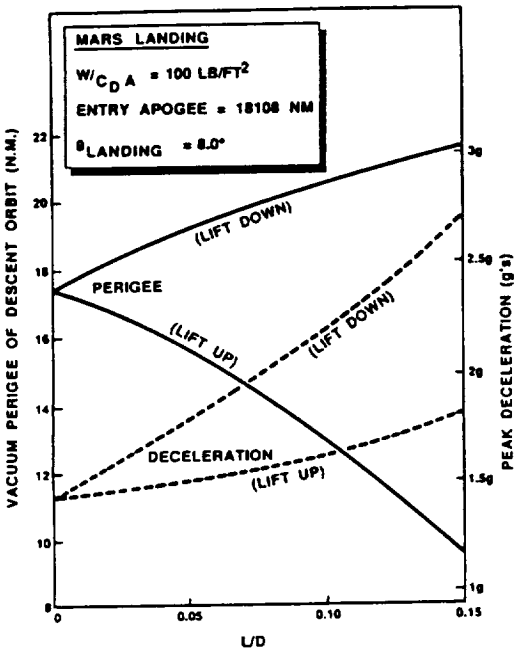

Figure 5.2-2 -
Mars Landing - L/D Parametrics

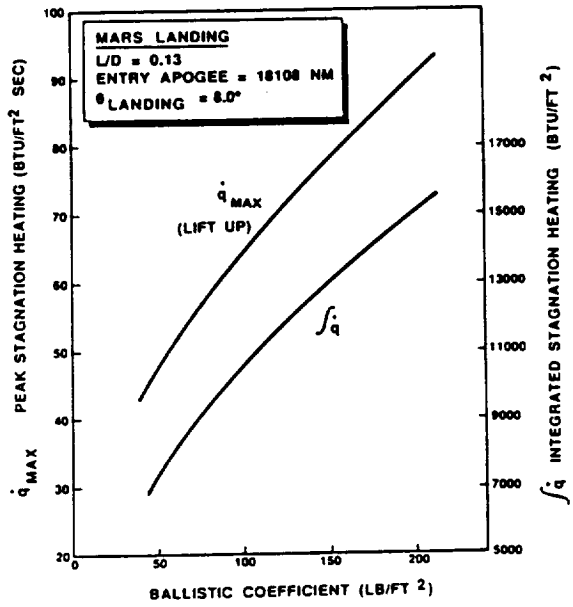

Figure 5.2-3 -
Mars Landing - Heating Parametrics

Figure 5.2-3 shows the peak stagnation and integrated heating encountered in the limiting lift up and lift down landing profiles. It is apparent that the thermal loads are also much smaller than those associated with Mars capture.

Time histories of key trajectory parameters are shown in Appendix C and D for the lift up and lift down Mars landing profiles.

5.3 Earth Capture Parametrics

Lift up and lift down extremum trajectory data is shown in Figures 5.3-1 and 5.3-2 for the Earth return aerocapture phase. The nominal hyperbolic encounter condition of $C_3 = 68$ km^2/Sec^2 is shown along with a more benign profile whose C_3 is 32 km^2/Sec^2. The post-aero apogee of 38484 nmi. is used as the target condition for both encounter conditions. Velocity reduction in the aeropass is 10370 fps for the $C_3 = 68$ encounter and 5880 fps for the $C_3 = 32$ orbit.

Control corridor widths are much wider for the higher C_3 at a given L/D (Figure 5.3-1). The larger velocity reduction results in a larger lift component which can be used for greater maneuverability. However, the faster entry condition results in much higher peak deceleration loads.

The heating information shown in Figure 5.3-2 is for the 68 km^2/sec^2 condition only and follows the same format shown in the previous sections.

Time histories of key parameters for lift up and lift down Earth captures are shown in Appendix E and F.

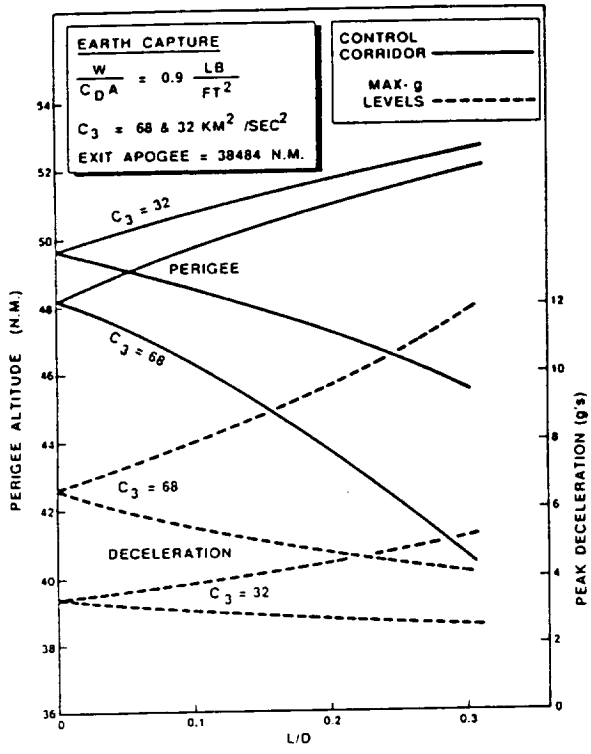

Figure 5.3-1 -
Earth Capture - L/D Parametrics

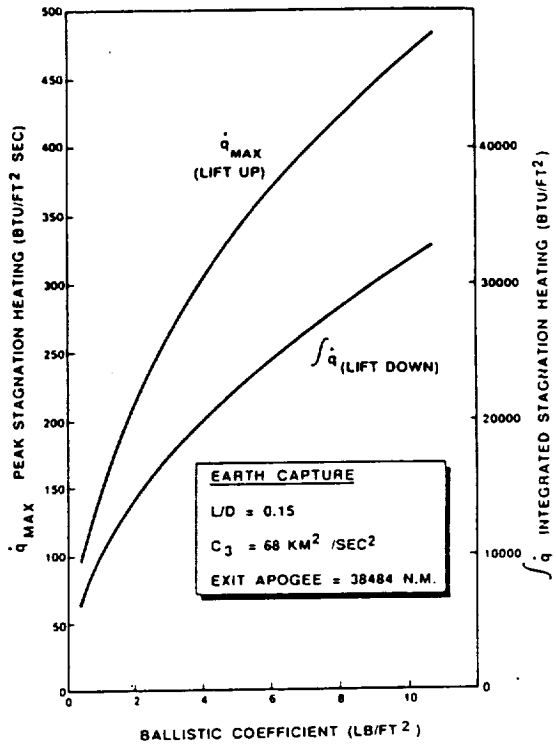

Figure 5.3-2 -
Earth Capture - Heating Parametrics

6.0 Error Analysis

The total magnitude of all errors affecting an aeroentry trajectory determines the amount of aerodynamic control required. Following the strategy developed in OTV Phase A studies (References 4, 5, 6), targeting errors are combined with aerodynamic variations to establish a control corridor width (Figure 6.0-1). This control corridor is bounded by lift up and lift down

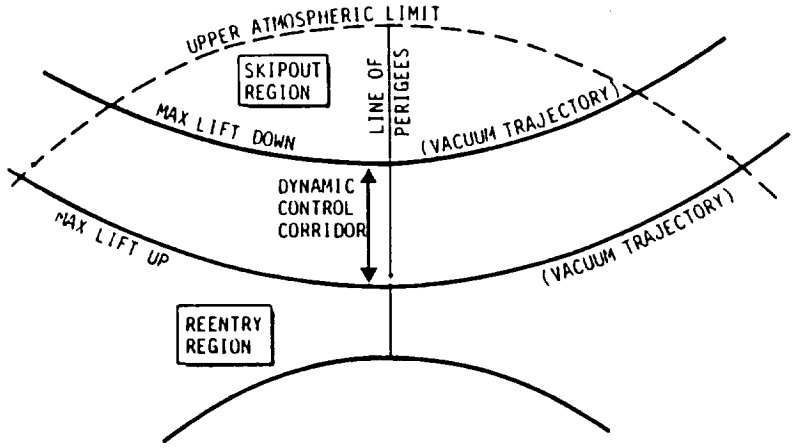

Figure 6.0-1 - Aerodynamic Control Corridor

limiting trajectories and thus describes the entry volume within which the vehicle is controllable. The control corridor size derived by this error analysis sets the vehicle's aerodynamic L/D requirements.

6.1 Interplanetary Navigation

Navigation accuracy is one of the primary drivers of aeroentry uncertainty. Operations remote from the Earth must rely on long-range radio tracking and celestial navigation for this function.

Very long base interferometry (VLBI) joins electrically the capabilities of a number of widely separated Earth tracking stations to achieve high state vector accuracies. The technique has been used in the Voyager project and will be used on Galileo. Position accuracies of 5 nmi. per A.U. separation from Earth should be achievable in the near future.

Once a spacecraft can optically detect a target planet, terminal navigation using onboard sensors can very accurately locate its position. Two techniques have been investigated. The first uses an onboard video camera (assumed to be part of the science payload) which photographs the planet as the encounter proceeds. This technique has been widely used in planetary missions (Mariner, Viking, Voyager) and yields about 1.0 nmi. position accuracy per 10,000 nmi. separation from the planet. Ultimately, an hour before entry, this technique can result in a 1.5 nmi. position accuracy for the baseline Mars encounter condition. For an aeroassisted mission this navigation process would have to be automated on-board to eliminate the delays associated with Earth-based processing.

The second technique is based on an autonomous stellar sextant package and has higher accuracies because of a wider effective field of view. The system uses two independently gimballed tracking telescopes linked to an onboard computer which contains stellar and planetary ephemeris data along with

atmospheric correction factors. Near-continuous navigation fixes are possible because the system can operate independently of the host vehicle's attitude. Based on data from the ANARS Space Sextant Program one could expect state vector accuracies on the order of 0.5 nmi. and 0.1 fps at the entry minus one hour point of Mars encounter.

In the entry error analysis a middle ground approach was chosen and the accuracies associated with the video navigation technique used (1.5 nmi. error at final correction an hour before entry).

6.2 Mars Capture Error Analysis

Table 6.2-1 summarizes the error analysis conducted to derive Mars capture control requirements. All errors are normalized into equivalent variations in perigee altitude which is the strongest driver to aeroentry uncertainty. The variables are catagorized into targeting errors and aerodynamic uncertainties.

The targeting errors result from inaccuracies in the execution of the final correction burn one hour before entry and include allocations for pointing error, cutoff error and navigation error. The pointing error of 0.1^{o} results from stellar update alignment errors and subsequent IMU drift which corrupts the desired pointing of the final correction. The velocity cutoff error of 0.33 fps results from onboard accelerometer errors and is a working figure derived from the OTV configuration. The navigation error is representative of video navigation capabilities as discussed in Section 6.1. These independent error contributions are RSS'ed together to yield a net perigee variation due to targeting errors of $\pm$1.52 nmi.

Table 6.2-1 - Mars Capture Error Analysis

	EQUIVALENT PERIGEE ERROR	
• TARGETING ERRORS (FINAL CORRECTION BURN AT ENTRY MINUS 1 HR)		
- POINTING ERROR	= 130 FT	±.1 DEG
- CUTOFF ERROR	= 1200 FT	.33 FPS ACCELEROMETER
- NAV ERROR	= 9100 FT	FROM 1.5 NM POSITION UNCERTAINTY
	750 FT	FROM 0.2 FPS VELOCITY UNCERTAINTY
• AERODYNAMIC VARIATION		
- ATMOSPHERIC UNCERTAINTY	= 18800 FT	± 50% DENSITY
- L/D UNCERTAINTY	= 10900 FT	± 2° AT 13° ANGLE OF ATTACK (± 30% L/D)
- BALLISTIC UNCERTAINTY	= 1600 FT	WT = ± 150 LB (RESIDUALS)
		C_D = ± 5% (STS/VIKING DATA) ± 8% $W/C_D A$
		A = ± 5%
• RSS	= ± 9210 FT	= ± 1.52 NM FROM TARGETING
	= ± 21800 FT	= ± 3.59 NM FROM AERODYNAMICS
	= ± 23700 FT	= ± 3.89 NM NET VARIATION

CONCLUSION: 10.3 N.M. CONTROL CORRIDOR REQUIRED TO COVER ERRORS WITH 33% MARGIN

The aerodynamic errors result from variations in the Mars atmospheric density as well as in vehicle aerodynamic properties during the entry phase. A Martian atmospheric variation of ± 50% in density is assumed (as compared with ± 30% for Earth applications) which is derived from the cool versus warm density models contained in the Mars reference atmosphere. The L/D uncertainty results from a vehicle trim attitude variability of ±2° in the continuum flow region of entry. The size of the variation is that derived for the OTV, when the Mars vehicle becomes better defined a similar derivation will be possible for its specific configuration. Finally, a ballistic uncertainty of ±8% is carried which also represents a quantity derived from the OTV. The RSS of the aerodynamic variations is ±3.59 nmi. in nominal perigee altitude.

When the targeting and aerodynamic errors are combined a net perigee variation of ±3.89 nmi. results. This variation in the aeroentry trajectory must be covered by the control capability of the vehicle in order to successfully accomplish the aeroassist. From experience with the OTV aeroentry process a 33% margin is added to the net variation to account for control lags. This results in a net control corridor requirement of 10.2 nmi. which then sets the L/D of the Mars entry vehicle at 0.2 using the parametric data contained in Figure 5.1-1.

6.3 Mars Landing Error Analysis

The Mars landing error analysis is summarized in Table 6.3-1. The same entry strategy is followed as in the Mars capture case with a final trajectory correction being performed an hour before entry. The same basic navigational capabilities are assumed even though the lander can benefit from several tracking revolutions in Martian orbit to produce a refined pre-deployment state vector. The same aerodynamic variations are used with their impact on perigee altitude changed because of the different aeroentry profile.

Table 6.3-1 - Mars Landing Error Analysis

	EQUIVALENT PERIGEE ERROR	
• TARGETING ERRORS (FINAL CORRECTION BURN AT ENTRY MINUS 1 HR)		
- POINTING ERROR	= 130 FT	±.1 DEG
- CUTOFF ERROR	= 1200 FT	.33 FPS ACCELEROMETER
- NAV ERROR	= 9100 FT	FROM 1.5 NM POSITION UNCERTAINTY
	750 FT	FROM 0.2 FPS VELOCITY UNCERTAINTY
• AERODYNAMIC VARIATION		
- ATMOSPHERIC UNCERTAINTY	= 14400 FT	± 50% DENSITY
- L/D UNCERTAINTY	= 15800 FT	± 2° AT 9° ANGLE OF ATTACK (± 30% L/D)
- BALLISTIC UNCERTAINTY	= 3500 FT	WT = ± 150 LB (RESIDUALS)
		C_D = ± 5% (STS/VIKING DATA) ± 8% $W/C_D A$
		A = ± 5%
• RSS	= ± 9210 FT	= ± 1.52 NM FROM TARGETING
	= ± 21700 FT	= ± 3.57 NM FROM AERODYNAMICS
	= ± 23500 FT	= ± 3.87 NM NET VARIATION

CONCLUSION: 5.22 N.M. CONTROL CORRIDOR REQUIRED TO COVER ERRORS WITH 33% MARGIN

The net variation in pre-entry vacuum perigee that results is ±3.92 nmi. which becomes ±5.22 nmi. with the addition of a 33% margin. Based on the parametric data contained in Figure 5.2-2 an L/D of 0.133 is required of the Mars lander. This amount of control is adequate to steer the lander to the required landing spot, 8° downrange of the entry orbital apsides, in the face of the defined dispersion set.

6.4 Earth Capture Error Analysis

This error analysis is summarized in Table 6.4-1. The principle difference between this analysis and that conducted for the Mars capture condition are as follows. Long-range GPS navigation accuracies reflect the

Table 6.4-1 - Earth Capture Error Analysis

	EQUIVALENT PERIGEE ERROR	
• TARGETING ERRORS (FINAL CORRECTION BURN AT ENTRY MINUS 1 HR)		
- POINTING ERROR	= 1095 FT	± .1 DEG
- CUTOFF ERROR	= 2217 FT	.33 FPS ACCELEROMETER
- NAV ERROR	= 899 FT	FROM 1020 FT POSITION UNCERTAINTY
	1342 FT	FROM 0.1 FPS VELOCITY UNCERTAINTY
• AERODYNAMIC VARIATION		
- ATMOSPHERIC UNCERTAINTY	= 5100 FT	± 30% DENSITY
- L/D UNCERTAINTY	= 7300 FT	± 2° AT 9° ANGLE OF ATTACK (± 30% L/D)
- BALLISTIC UNCERTAINTY	= 2000 FT	WT = ± 150 LB (RESIDUALS)
		C_D = ± 5% (STS/VIKING DATA) ± 8% $W/C_D A$
		A = ± 5%
• RSS	= ± 3000 FT	= ± 0.49 NM FROM TARGETING
	= ± 10300 FT	= ± 1.69 NM FROM AERODYNAMICS
	= ± 10700 FT	= ± 1.76 NM NET VARIATION

CONCLUSION: 4.68 N.M. CONTROL CORRIDOR REQUIRED TO COVER ERRORS WITH 33% MARGIN

acquisition of the Earth-based NAVSAT constellation in the final day before entry and are of a higher quality than those resulting from stellar sightings alone. The atmospheric density variations are ±30% (as opposed to the Martian ±50%) because of the Earth's better data base and ground based sensing capabilities. The combination of errors yields a net ±1.76 nmi. variation which expands to a ±2.34 nmi. control corridor requirement with the addition of a 33% margin factor. Using the parametric data in Figure 5.3-1 this sets an Earth capture L/D of 0.15 for the nominal C_3 of 68. For the lower C_3 of 32 an L/D of 0.23 would be required.

7.0 Aerobrake Materials and Structural Analyses

Having set the lift characteristics of the two aerobrakes, the TPS and structural characteristics may then be determined. Brake sizing is based on projected 1990's TPS heat flux limits for rigid surface insulations (RSI) and flex surface insulations (FSI) as well as the prevention of direct flow impingement to the afterbody of the vehicle. Complete details of the computational procedure and data base used are given in References 4 & 5. Nonequilibrium radiative emission rates are based on earth reentry predictions and are used in determining heating environments for all three aeromaneuvers. Stagnation point convective heating rates are based on a modified Fay-Riddell method. Real gas effects on aeroshell heating and dissociation impacts on aerocharacteristics are not included.

7.1 Mars and Earth Capture Brake

The use of a common aerobrake to perform Mars and Earth capture saves on weight by eliminating hardware duplication. The design drivers for sizing are picked from the most stressful of the two flight phases. The Mars capture phase sets afterbody impingement criteria while the Earth capture sets thermal and loading criteria.

To prevent afterbody flow impingement in the Mars capture phase a 104 foot diameter, 70° conical brake would be required. Use of this same brake size for Earth aerocapture would limit the ballistic coefficient to 10.0, due to the 50 BTU/ft^2-sec heat flux limit of rigid surface insulation (RSI). To achieve this ballistic coefficient the Earth return vehicle's weight would have to be reduced to 133000 lb. by jettisoning some of the vehicle modules just prior to Earth entry. In addition, edge heating exceeds FSI capabilities and the entire brake would have to be made of the heavier RSI.

A resizing process was performed to allow the return to Earth of the complete Mars vehicle, weighing 163,000 lb. This includes the Lab/Hab modules, the MEM 2nd stage, and the Mars escape stage (including 7,000 lb. of propellant). The brake was sized to allow FSI to be used on the periphery of the brake to save weight. The center of the brake uses RSI and was constrained to a diameter of 25 feet to allow intact delivery to LEO using the shuttle aft cargo carrier. Results of the analysis showed that a 142 foot diameter brake was required for the demanding Earth aerocapture phase.

The thermal design quantities are peak stagnation point heating of 40.3 BTU/ft^2 sec and integrated heating of 3254 BTU/ft^2 achieved in Earth capture. These levels require a 0.69 inch layer of RSI for the hard shell nose cap. The RSI/FSI interface location sees maximum heating values of 35.0 BTU/ft^2-sec (peak) and 2908 BTU/ft^2 (integrated) which sets the FSI blanket thickness at 0.40 inches. These heating values are normalized to the capture brake's nose radius of 35.5 ft.

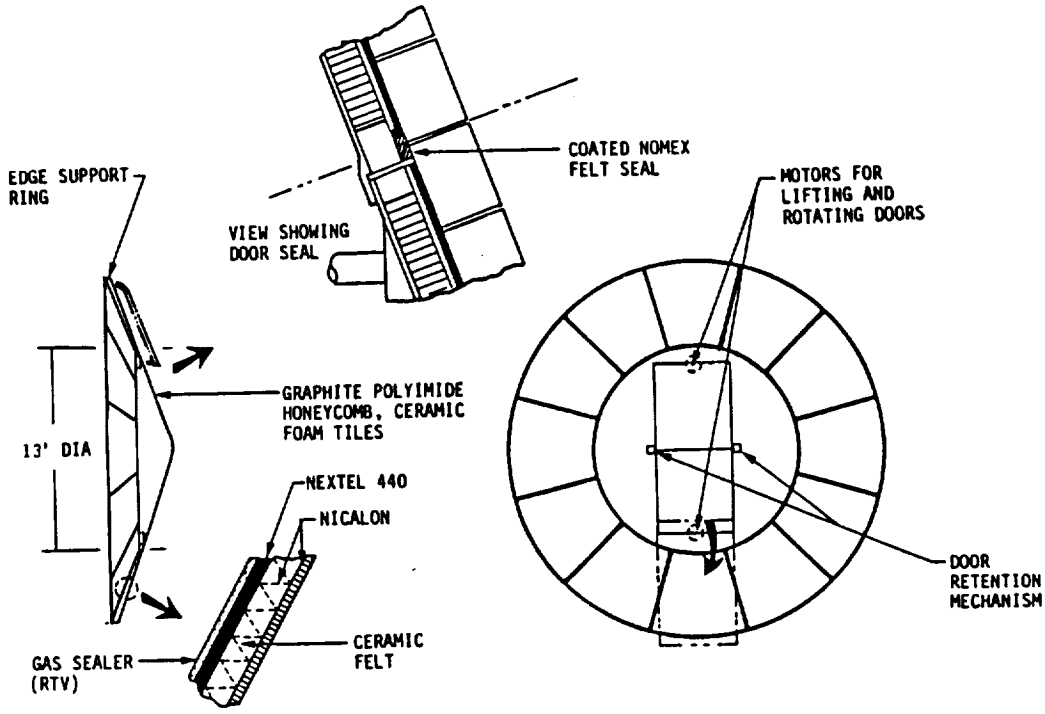

Figure 7.1-1 - Mars/Earth Capture Brake Overview

The support structure requirements are set by the peak g-loading of the strenuous Earth capture. Utilizing the space based OTV aerobrake as a baseline, structural scaling factors were derived which accounted for size and loads. The results of this analysis show a net structural weight (excluding TPS) for the Mars/Earth capture brake of 11032 lbs. The center core section contains doors through which the Mars escape stage engine bells protrude during non-aerobraked portions of flight. An overview layout of the brake's construction is shown in Figure 7.1-1. Other characteristics of the brake are summarized in Table 7.1-1.

Table 7.1-1 - Aerobrake Data

	MARS CAPTURE	MARS LANDING	EARTH CAPTURE
VEHICLE WEIGHT	465300 LB	157500 LB	163000 LB
L/D	0.2	0.133	0.15
ANGLE OF ATTACK	12.42 DEG	8.28 DEG	9.33 DEG
AEROBRAKE DIAMETER	142 FT	36 FT	142 FT
BALLISTIC COEFFICIENT	19.3 LB/FT2	100 LB/FT2	6.6 LB/FT2
PEAK LOADING	4.9 g's	2.5 g's	8.3 g's
NUMBER OF RIBS	38	12	38
AEROBRAKE TOTAL WEIGHT (*)	23371 LB (*)	1392 LB (*)	23371 LB (*)
RSI WEIGHT	401 LB	0	401 LB
FSI WEIGHT	8890 LB	786 LB	8890 LB
STRUCTURAL WEIGHT	11032 LB	424 LB	11032 LB

(* NOTE: AEROBRAKE TOTAL WEIGHT INCLUDES A 15% CONTINGENCY)

It should be noted that this brake is severely driven by the Earth encounter C_3 of 68 km^2/sec^2. The more benign encounter condition of C_3 = 32 km^2/sec^2 will result in an overall brake weight reduction of at least 30%.

7.2 Mars Landing Aerobrake

The thermal and structural analysis of the Mars landing aerobrake was conducted in the same manner as described in the previous section. Because the thermal and deceleration loads are smaller the brake can be much lighter.

Afterbody impingement considerations for the MEM set a minimum brake diameter at 36 ft. At this size and based on an entry weight of 157,500 lb a ballistic coefficient of 100.0 results. When the parametric heating data is normalized to a nose radius of 9 ft, a peak stagnation heating of 17.4 BTU/ft^2 sec and an integrated heating of 2864 BTU/ft^2 results. At these heating levels an all-FRI fabric brake is possible whose TPS thickness is 0.65 inches.

Structural analysis shows that 12 ribs are adequate to support the high temperature ceramic fabric, with a total support structure weight of 424 lb. Because the brake will be jettisoned prior to the ignition of the terminal descent rockets, no engine doors are required. The characteristics of this brake are also summarized in Table 7.1-1.

8.0 Conclusions

The concept of a low L/D, ceramic fabric aerobrake developed in the OTV Phase A has been applied to a manned Mars mission. The resulting vehicle configuration is shown in Figure 8.0-1. The large Mars/Earth capture brake, which is permanently deployed, is shown on the left. The Mars excursion module is shown on the right in its trans-Mars configuration. The MEM's all-fabric brake is folded up in transit to prevent aerodynamic impingement during Mars aerocapture. Once in Mars orbit this brake is deployed in preparation for landing. Upon return to the Earth the entire remaining stack, consisting of the Mars escape stage, Lab/Hab modules, and the MEM stage 2 is aerocaptured by reusing the large brake.

Potential subjects for a follow-on to this effort would be: 1) a look at a reduced Earth entry velocity to allow a lighter capture brake, 2) better characterization of the Mars entry landing profile (including terminal landing constraints), 3) more detailed structural analysis of the large capture brake, and 4) techniques for reducing g-loads in the C_3=68 Earth capture.

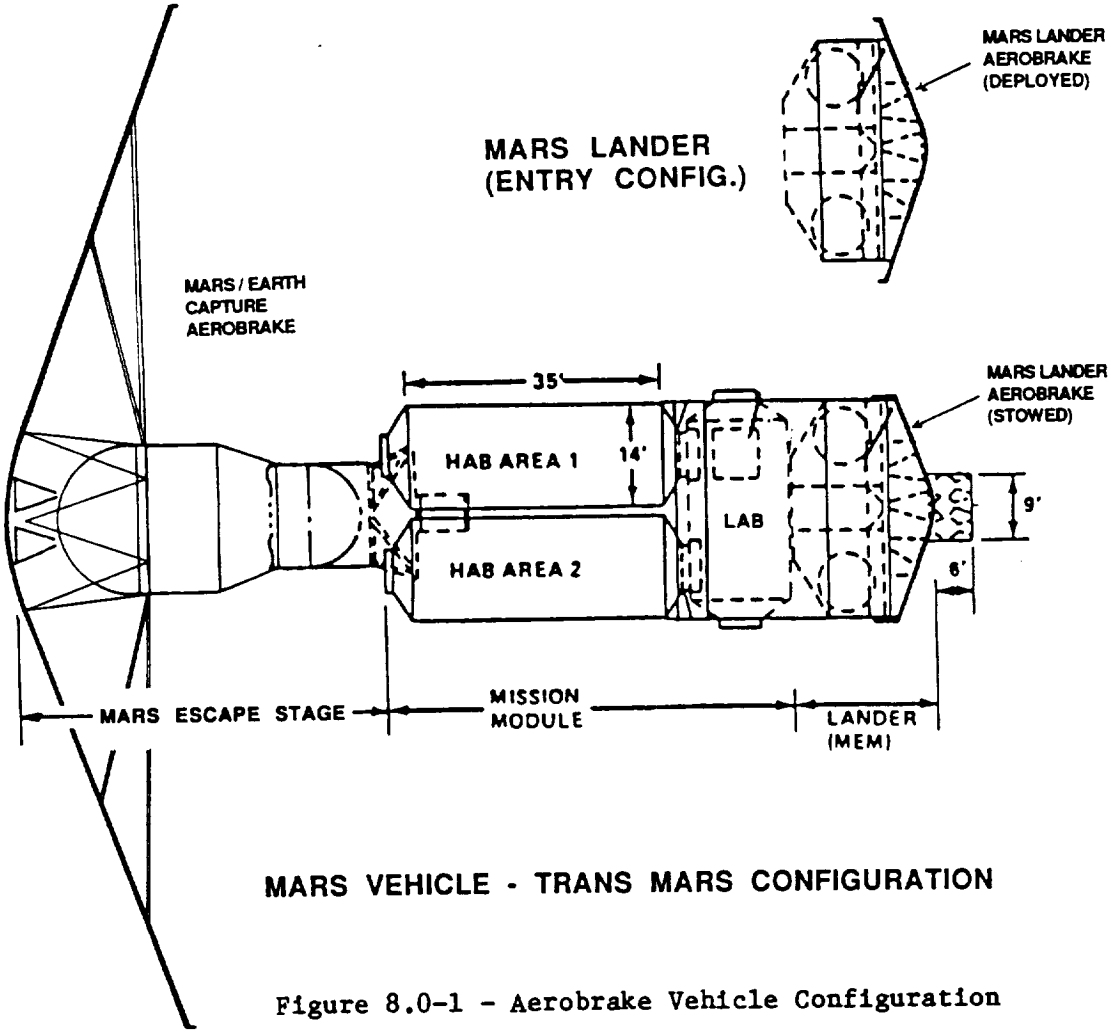

Figure 8.0-1 - Aerobrake Vehicle Configuration

References

1. Butler, John M.
"Mars Missions and Bases - A Recent Look"
George C. Marshall Space Flight Center, 1986

2. Kliore, A., et al
"The Mars Reference Atmosphere"
COSPAR - Jet Propulsion Laboratory Report, Innsbruck, Austria, 1978

3. Martin Marietta
"Viking Aerodynamics Data Book"
TR-3709014/NAS1-9000
December 1974

4. Martin Marietta
"Orbital Transfer Vehicle Concept Definition and System Analysis Study-Final Review"
MCR-85 2601/NAS8-36108
Marshall Space Flight Center, Huntsville, Alabama, August 1985

5. Martin Marietta
"Orbital Transfer Vehicle Concept Definition and System Analysis Study - Contract Extention - Final Review"
MCR-86/NAS8-36108/DR-3
Marshall Space Flight Center, Huntsville, Alabama, July 1986

6. Willcockson, William H.
"OTV Aeroassist with Low L/D"
IAF-86-115, 37th Congress of the International Astronautical Federation, Innsbruck, Austria, October 1986

APPENDIX A

OPEN-LOOP AEROPASS SIMULATION

MARS CAPTURE

CONTINUOUS LIFT UP

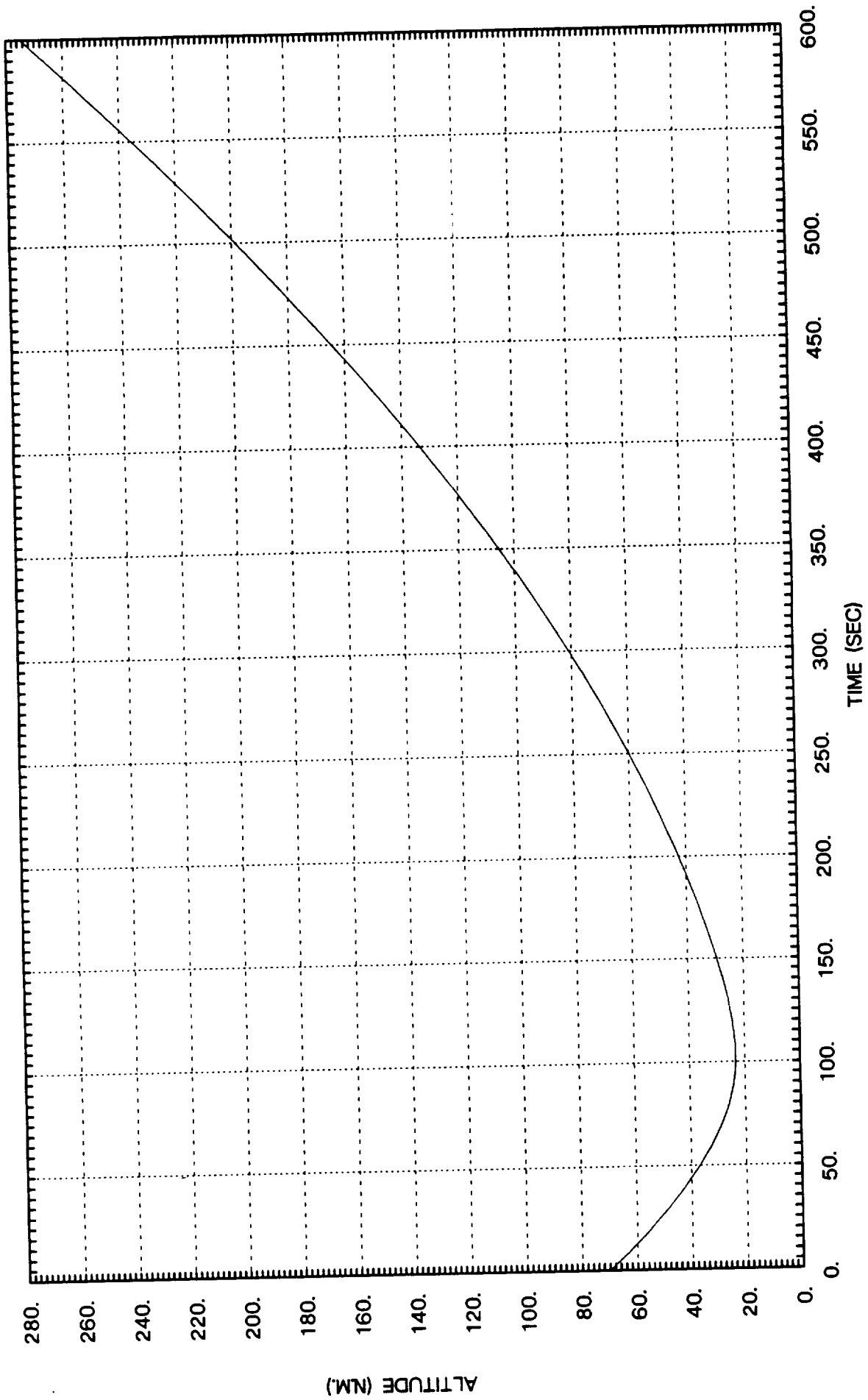
ALTITUDE (NM.)
280.
260.
240.
220.
200.
180.
160.
140.
120.
100.
80.
60.
40.
20.
0.
TIME (SEC)
0.
50.
100.
150.
200.
250.
300.
350.
400.
450.
500.
550.
600.

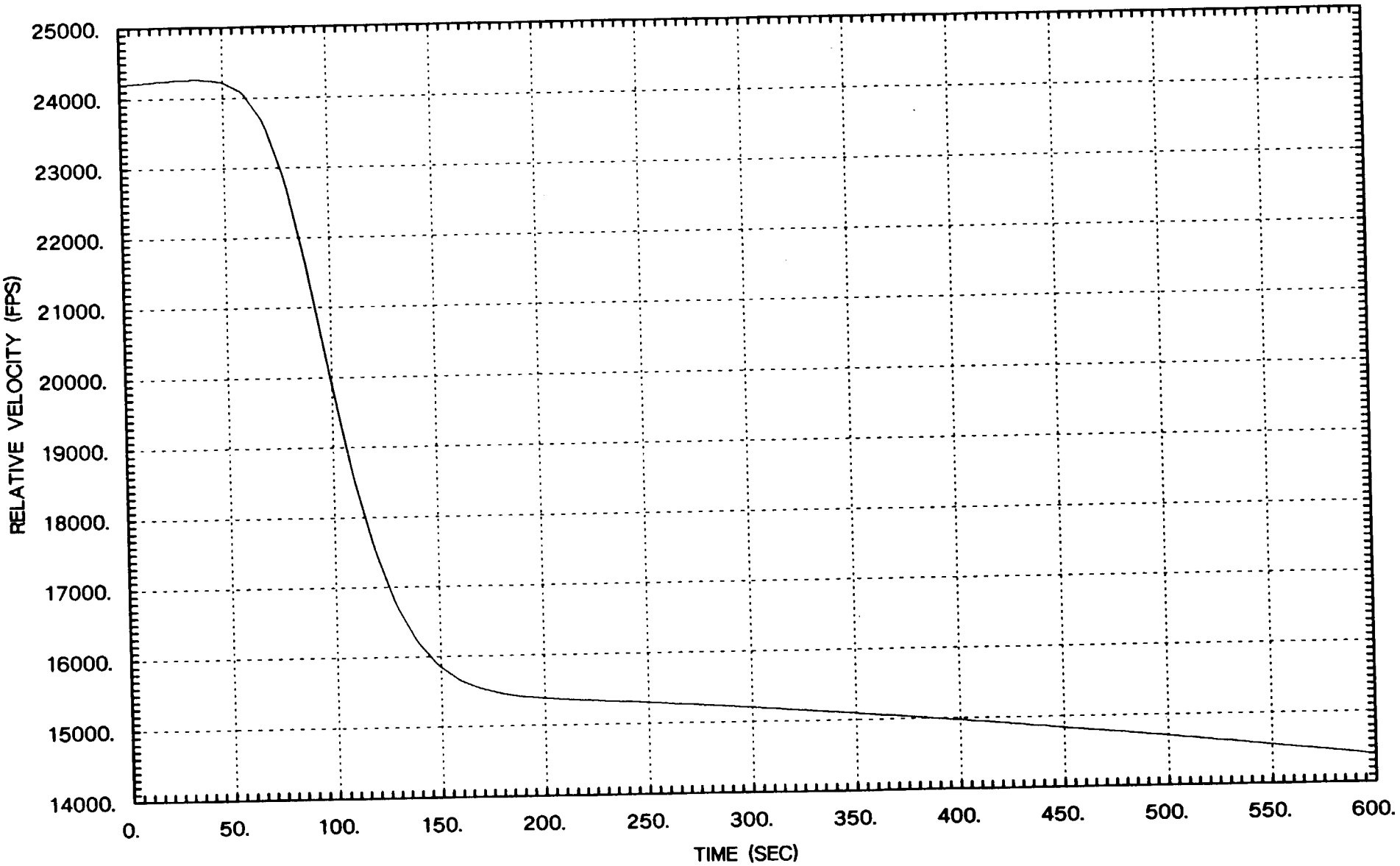
25000.
24000.
23000.
22000.
21000.
20000.
19000.
18000.
17000.
16000.
15000.
14000.
RELATIVE VELOCITY (FPS)
0.
50.
100.
150.
200.
250.
300.
350.
400.
450.
500.
550.
600.
TIME (SEC)

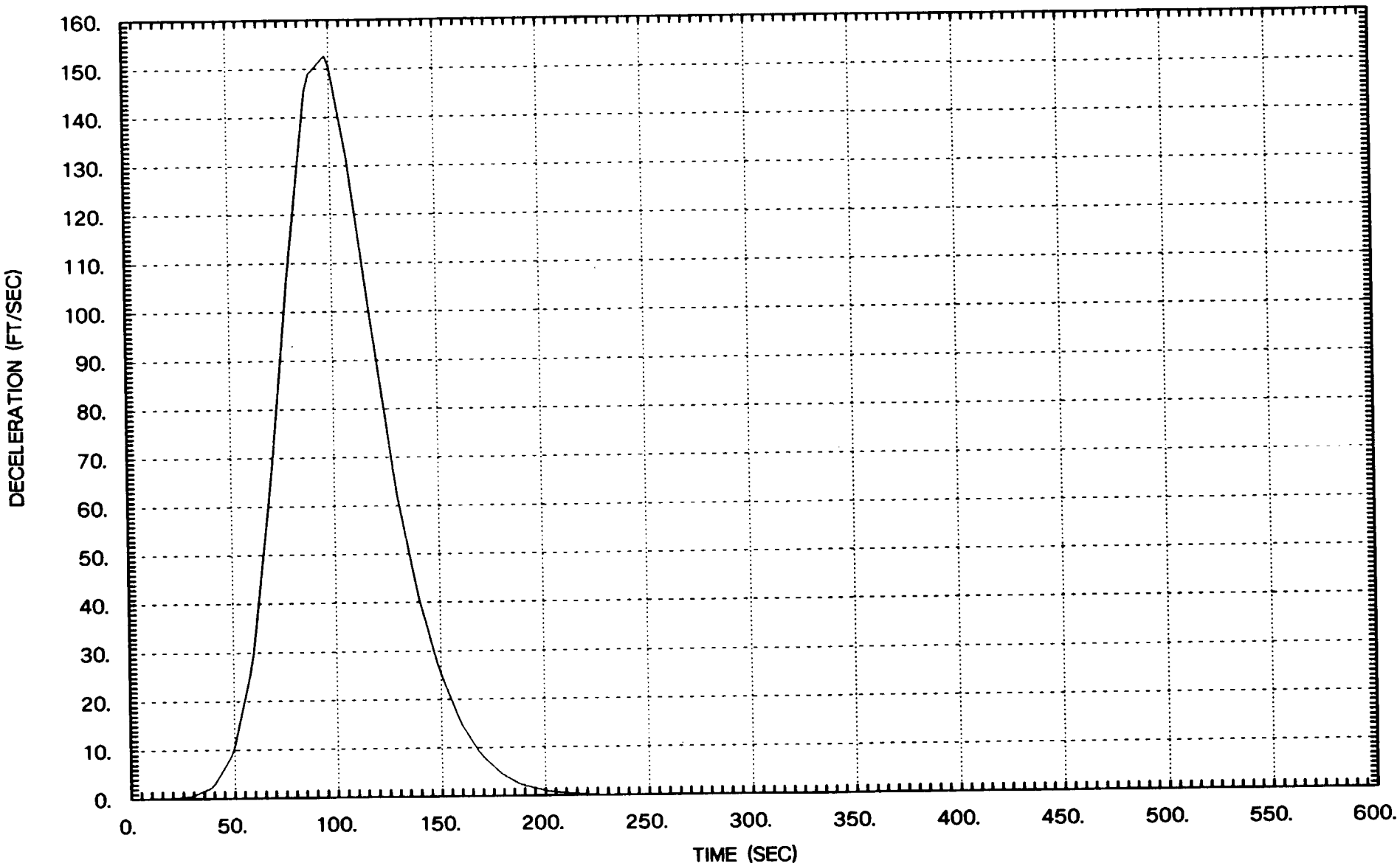
DECELERATION (FT/SEC)
160.
150.
140.
130.
120.
110.
100.
90.
80.
70.
60.
50.
40.
30.
20.
10.
0.
0.
50.
100.
150.
200.
250.
300.
350.
400.
450.
500.
550.
600.
TIME (SEC)

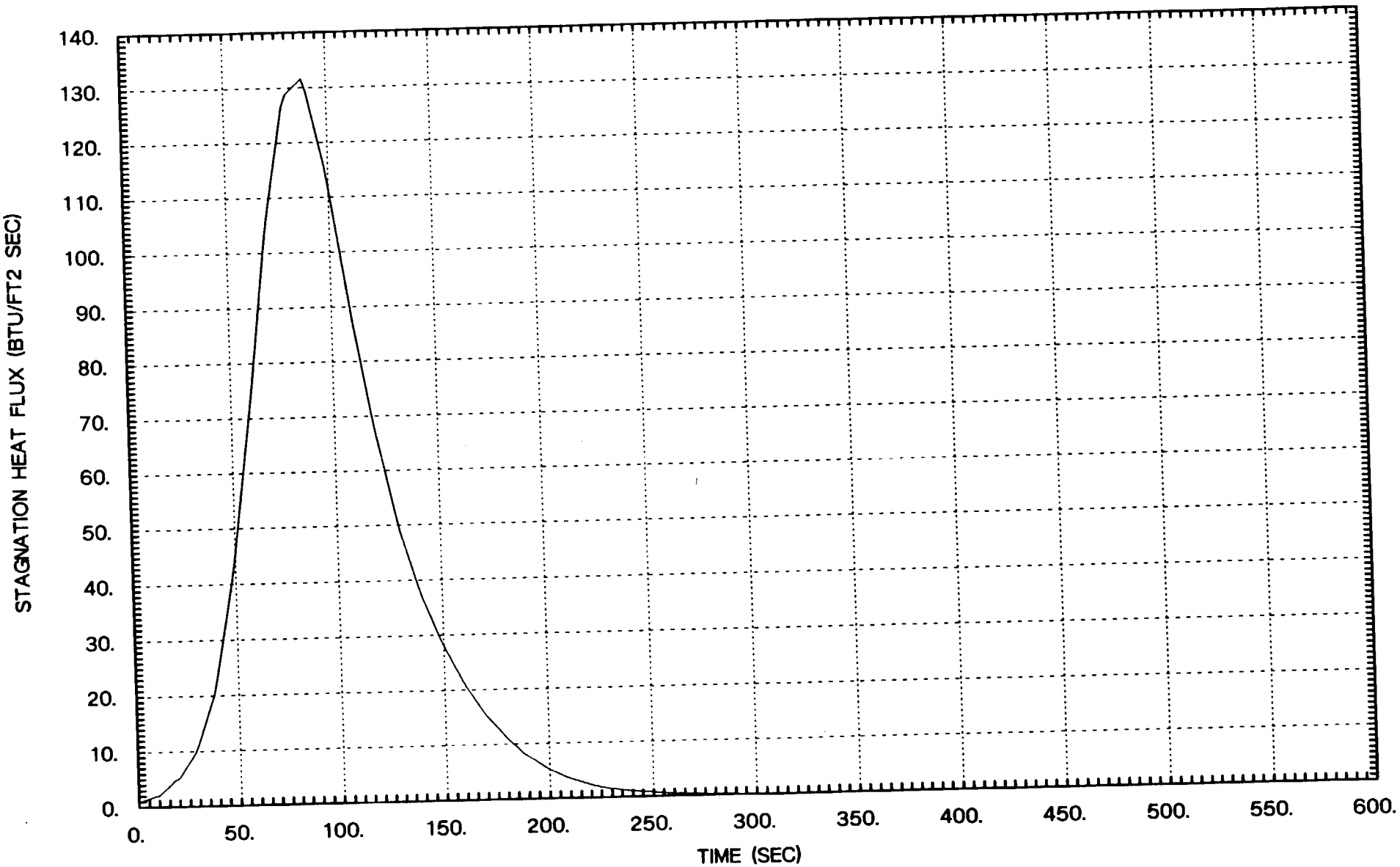
STAGNATION HEAT FLUX (BTU/FT2 SEC)
140.
130.
120.
110.
100.
90.
80.
70.
60.
50.
40.
30.
20.
10.
0.
0.
50.
100.
150.
200.
250.
300.
350.
400.
450.
500.
550.
600.
TIME (SEC)

APPENDIX B

OPEN-LOOP AEROPASS SIMULATION

MARS CAPTURE

CONTINUOUS LIFT DOWN

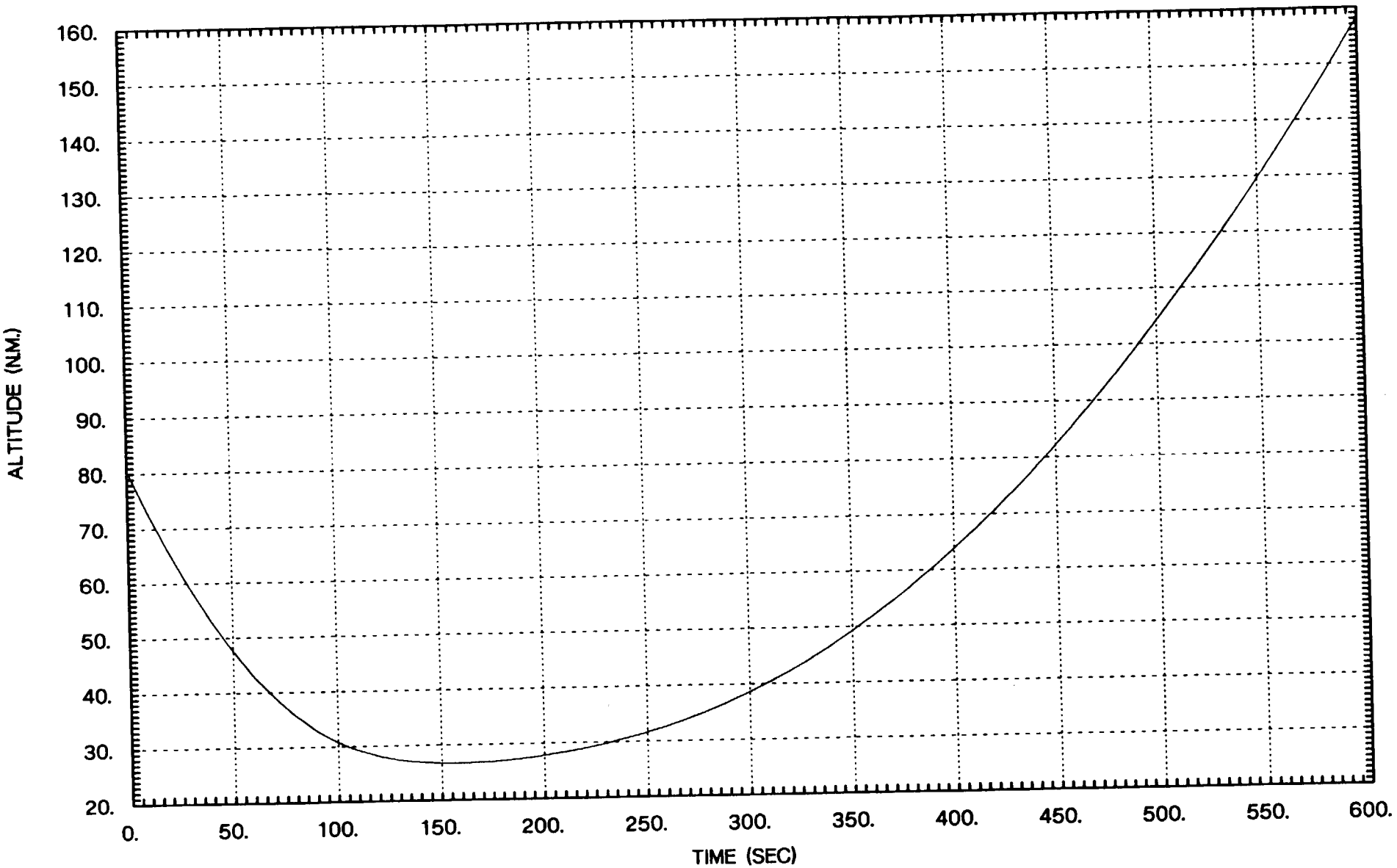
160.
150.
140.
130.
120.
110.
100.
90.
80.
70.
60.
50.
40.
30.
20.
ALTITUDE (N.M.)
0.
50.
100.
150.
200.
250.
300.
350.
400.
450.
500.
550.
600.
TIME (SEC)

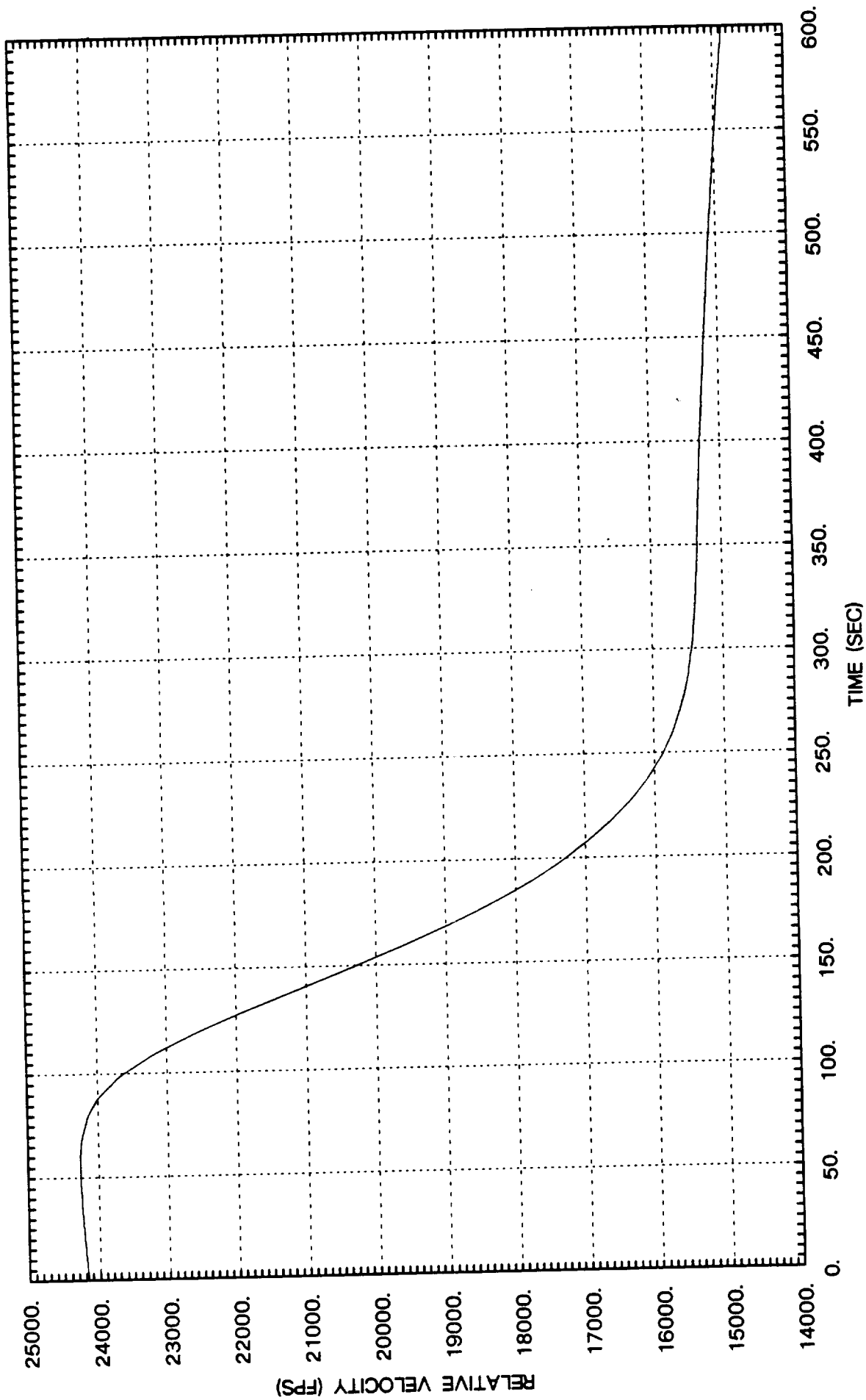
RELATIVE VELOCITY (FPS)
25000.
24000.
23000.
22000.
21000.
20000.
19000.
18000.
17000.
16000.
15000.
14000.
0.
50.
100.
150.
200.
250.
300.
350.
400.
450.
500.
550.
600.
TIME (SEC)

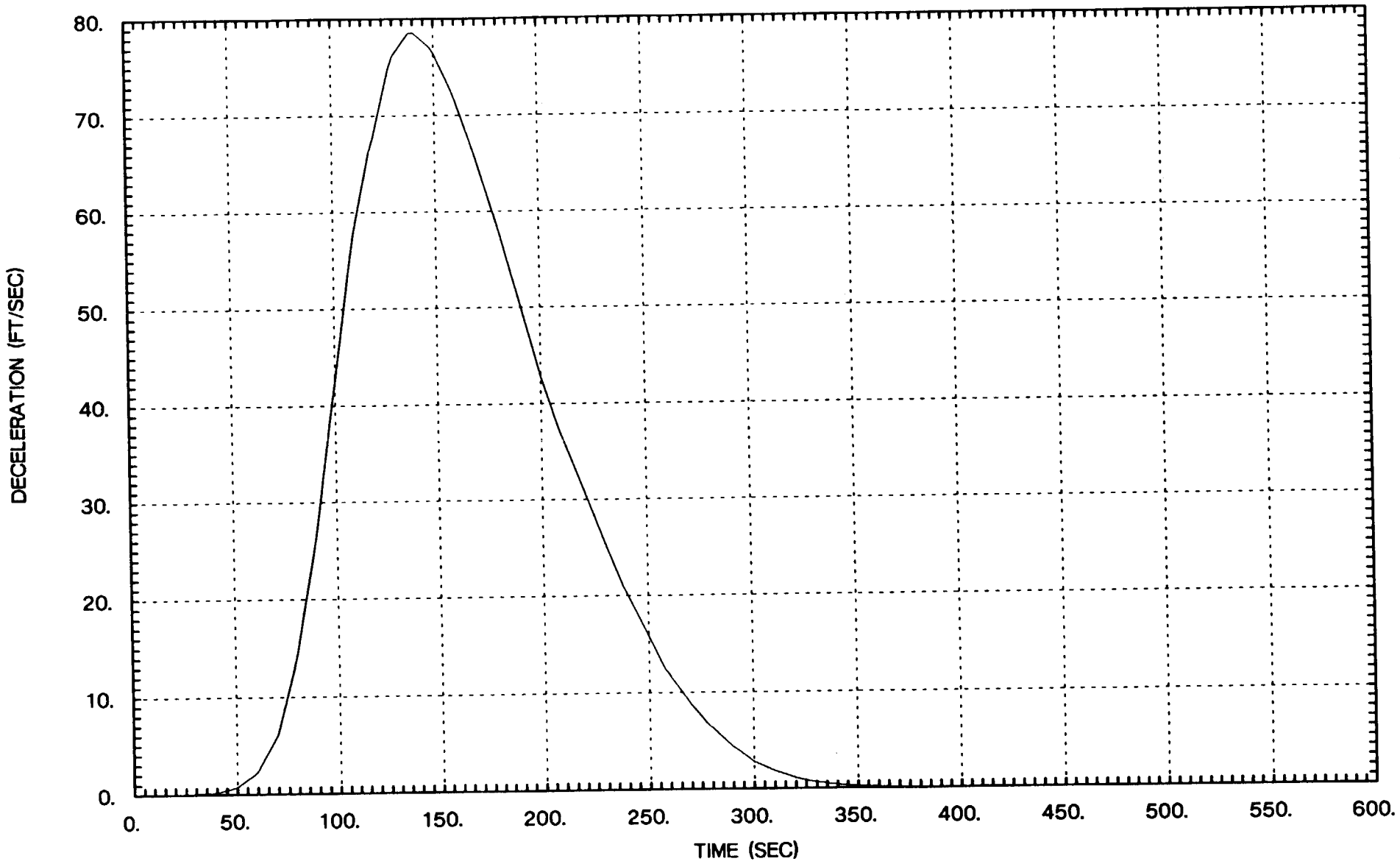
80.
70.
60.
50.
40.
30.
20.
10.
0.
DECELERATION (FT/SEC)
0.
50.
100.
150.
200.
250.
300.
350.
400.
450.
500.
550.
600.
TIME (SEC)

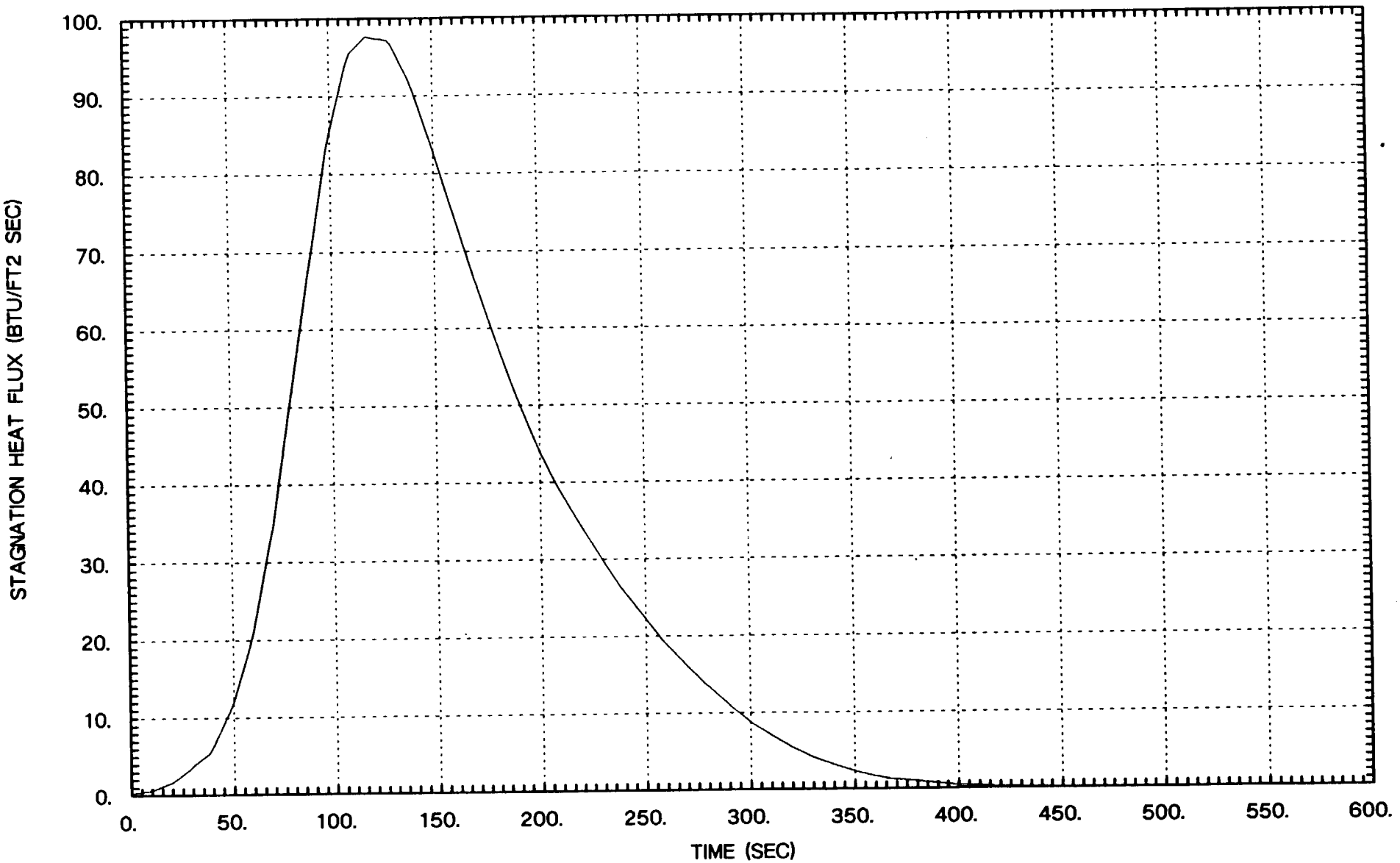
STAGNATION HEAT FLUX (BTU/FT2 SEC)
100.
90.
80.
70.
60.
50.
40.
30.
20.
10.
0.
0.
50.
100.
150.
200.
250.
300.
350.
400.
450.
500.
550.
600.
TIME (SEC)

APPENDIX C

OPEN-LOOP AEROPASS SIMULATION

MARS LANDING

CONTINUOUS LIFT UP

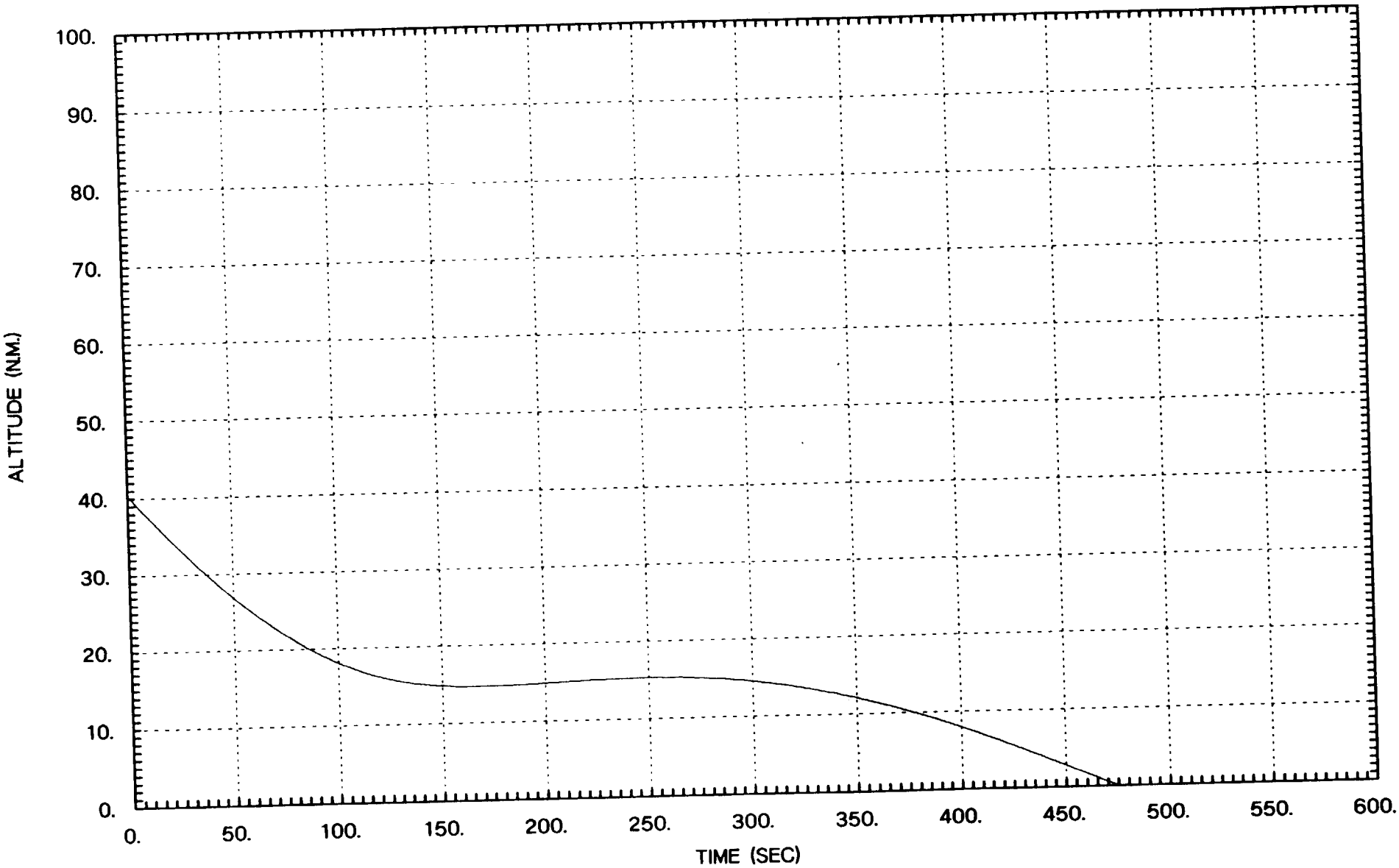
100.
90.
80.
70.
60.
50.
40.
30.
20.
10.
0.
ALTITUDE (N.M.)
0.
50.
100.
150.
200.
250.
300.
350.
400.
450.
500.
550.
600.
TIME (SEC)

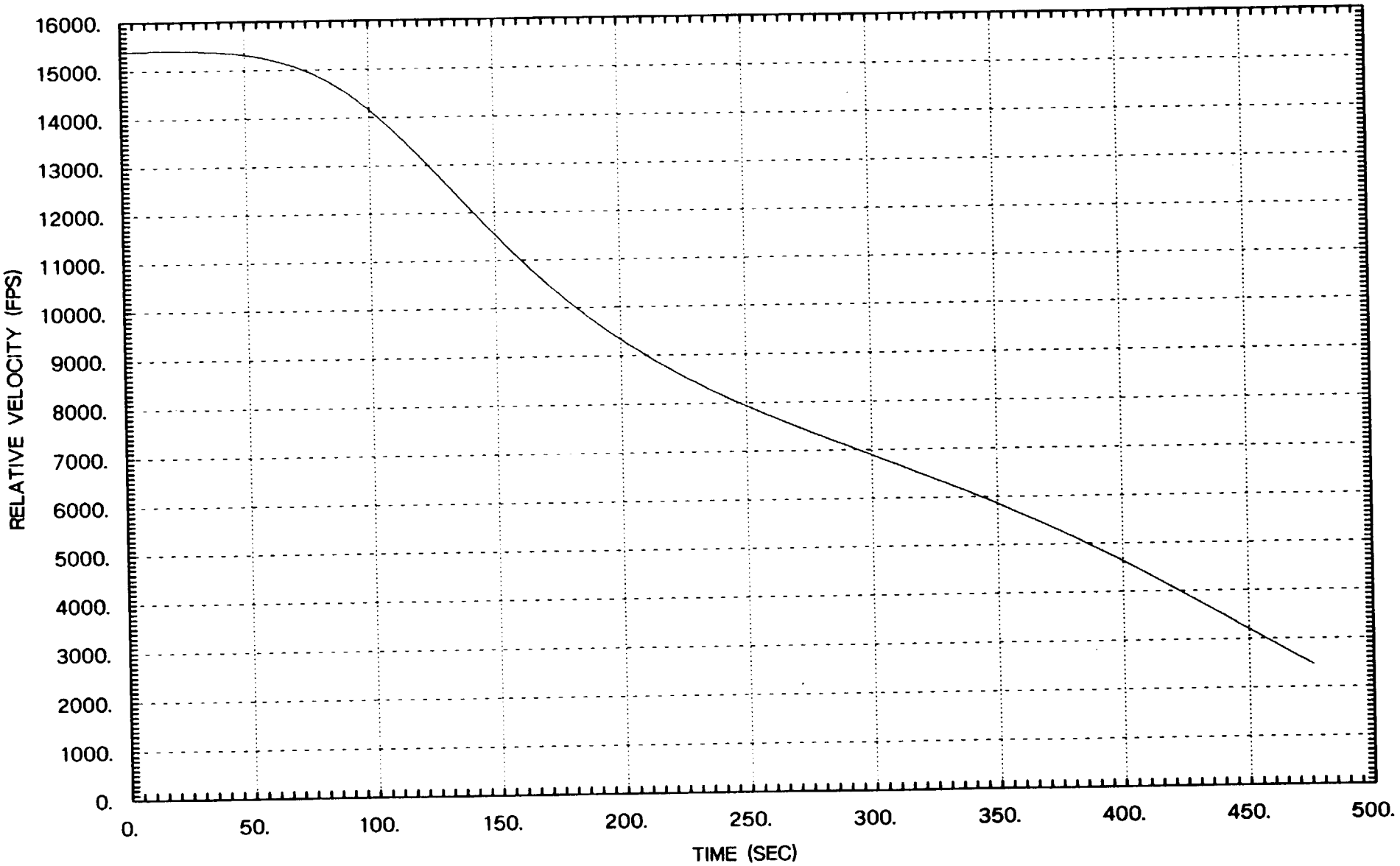
16000.
15000.
14000.
13000.
12000.
11000.
10000.
9000.
8000.
7000.
6000.
5000.
4000.
3000.
2000.
1000.
0.
RELATIVE VELOCITY (FPS)
0.
50.
100.
150.
200.
250.
300.
350.
400.
450.
500.
TIME (SEC)

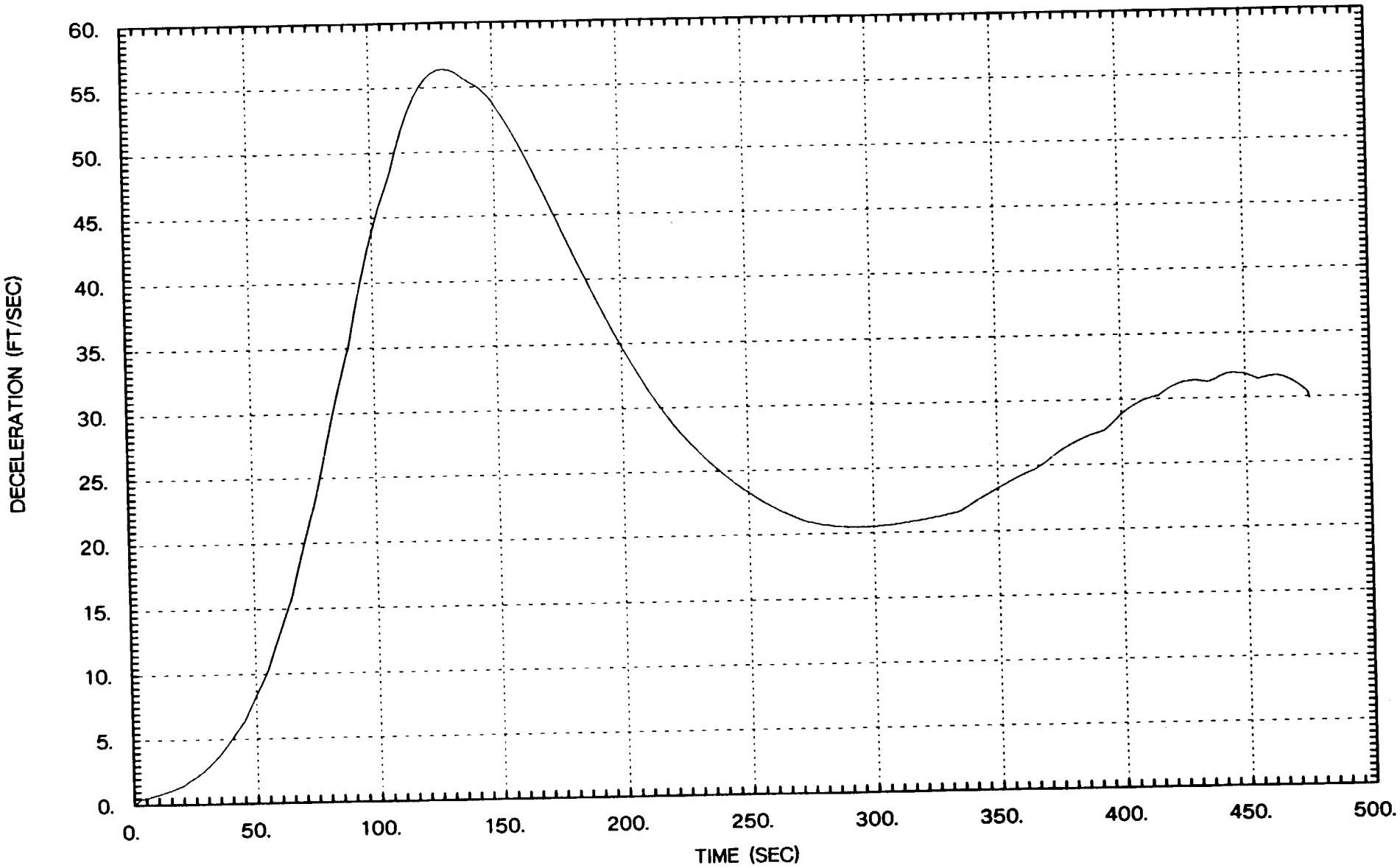
60.
55.
50.
45.
40.
35.
30.
25.
20.
15.
10.
5.
0.
DECELERATION (FT/SEC)
0.
50.
100.
150.
200.
250.
300.
350.
400.
450.
500.
TIME (SEC)

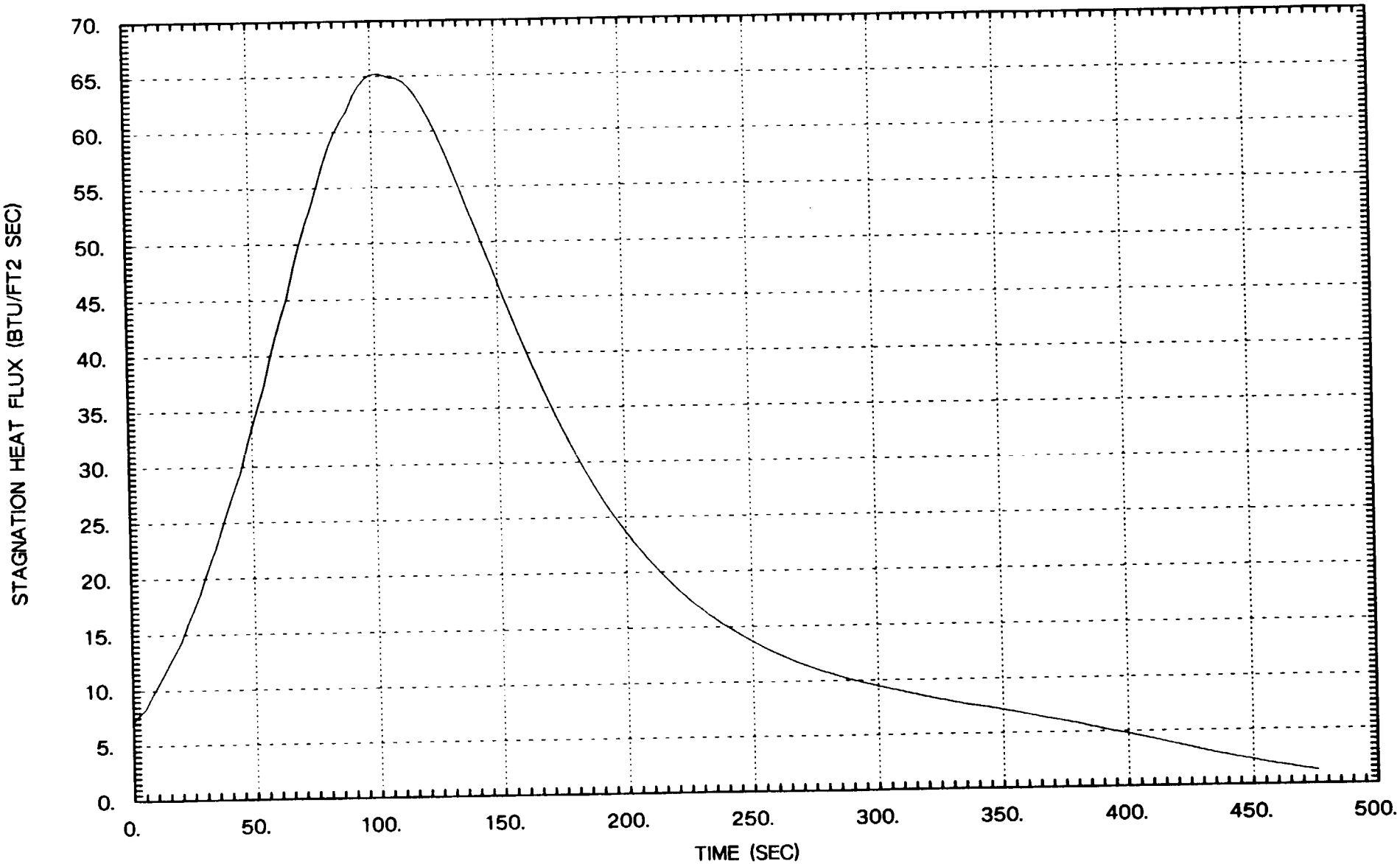
STAGNATION HEAT FLUX (BTU/FT2 SEC)
70.
65.
60.
55.
50.
45.
40.
35.
30.
25.
20.
15.
10.
5.
0.
0.
50.
100.
150.
200.
250.
300.
350.
400.
450.
500.
TIME (SEC)

APPENDIX D

OPEN-LOOP AEROPASS SIMULATION

MARS LANDING

CONTINUOUS LIFT DOWN

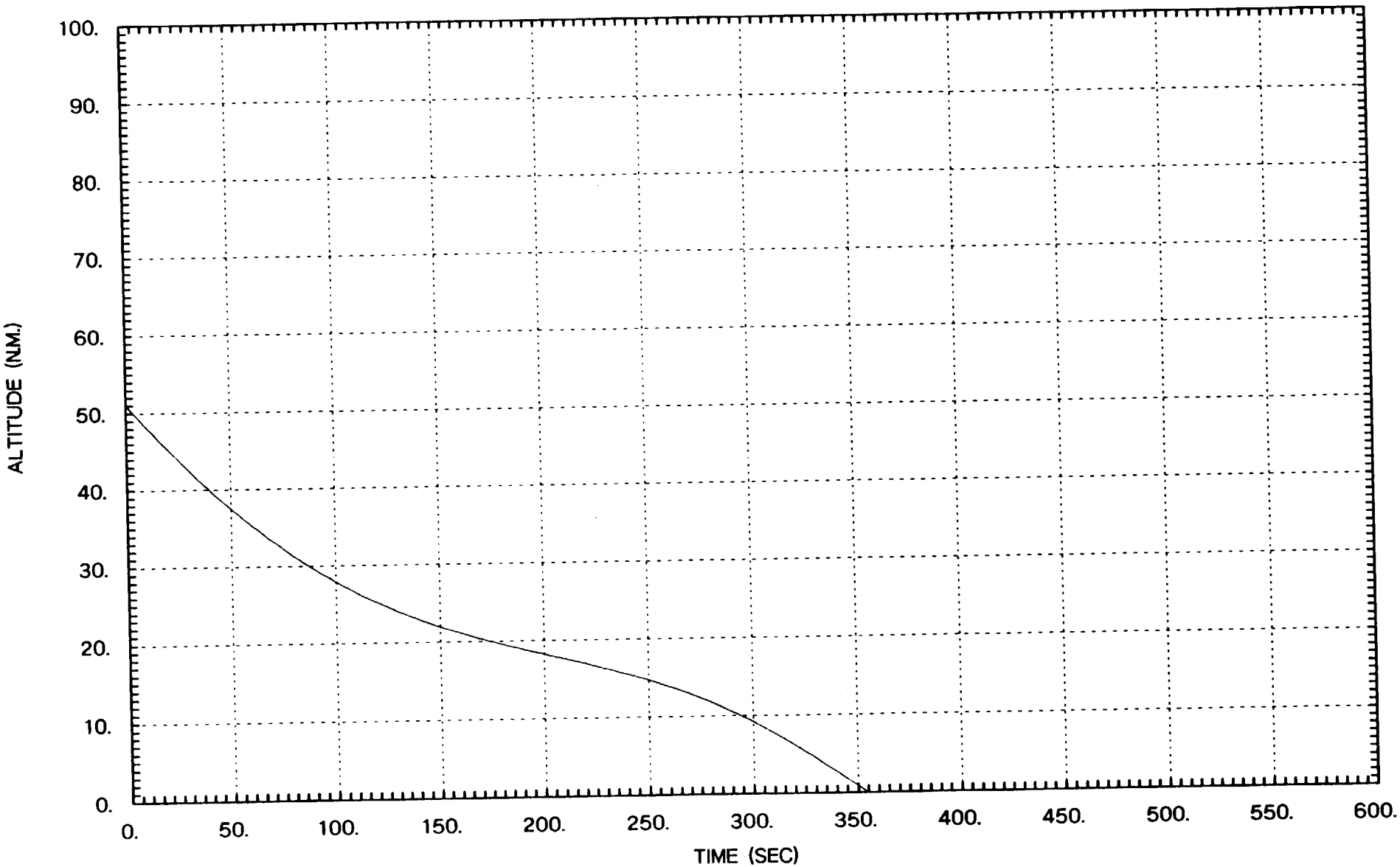
100.
90.
80.
70.
60.
50.
40.
30.
20.
10.
0.
ALTITUDE (N.M.)
0.
50.
100.
150.
200.
250.
300.
350.
400.
450.
500.
550.
600.
TIME (SEC)

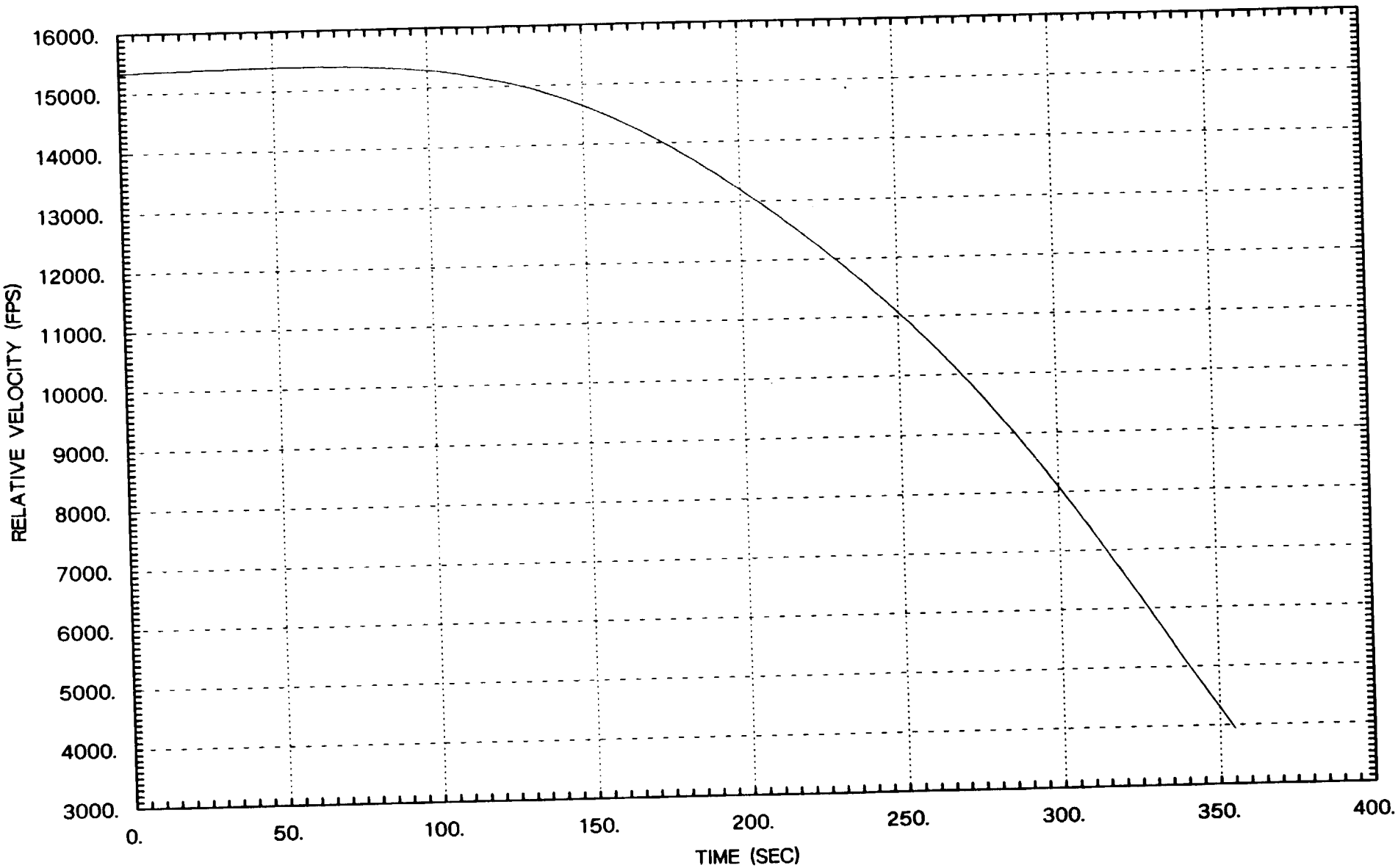
16000.
15000.
14000.
13000.
12000.
11000.
10000.
9000.
8000.
7000.
6000.
5000.
4000.
3000.
RELATIVE VELOCITY (FPS)
0.
50.
100.
150.
200.
250.
300.
350.
400.
TIME (SEC)

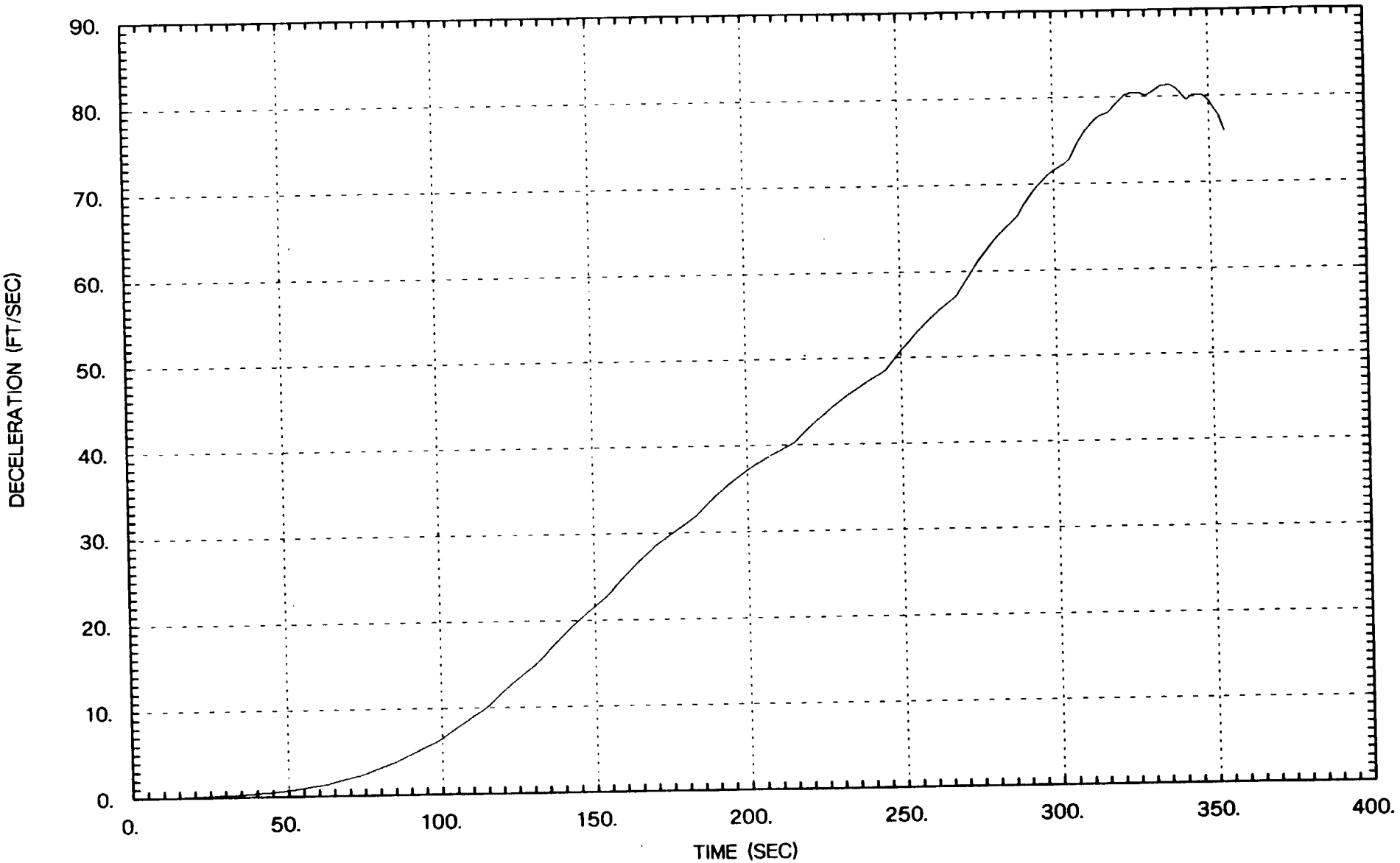
90.
80.
70.
60.
50.
40.
30.
20.
10.
0.
DECELERATION (FT/SEC)
0.
50.
100.
150.
200.
250.
300.
350.
400.
TIME (SEC)

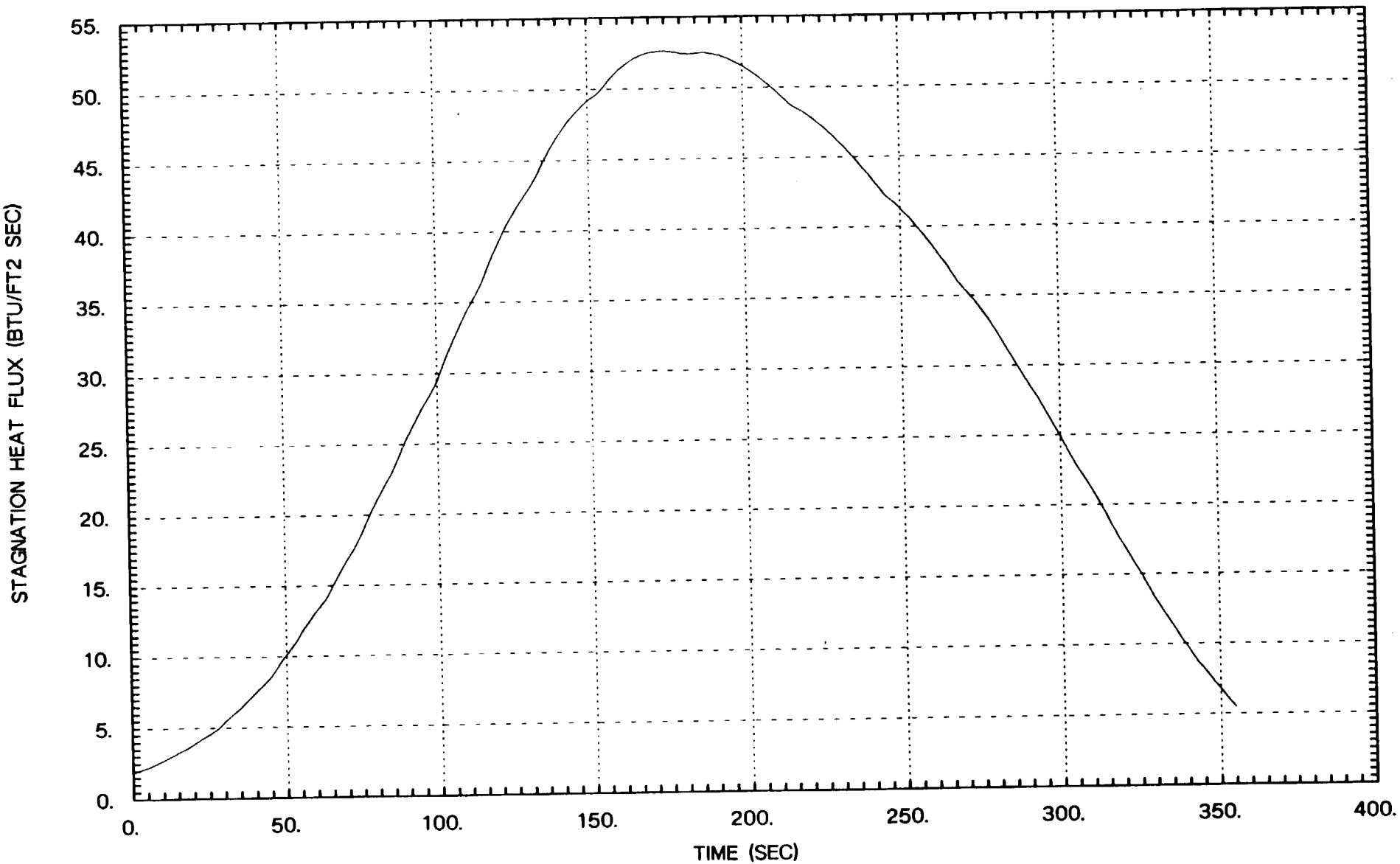
STAGNATION HEAT FLUX (BTU/FT2 SEC)
55.
50.
45.
40.
35.
30.
25.
20.
15.
10.
5.
0.
0.
50.
100.
150.
200.
250.
300.
350.
400.
TIME (SEC)

APPENDIX E

OPEN-LOOP AEROPASS SIMULATION

EARTH CAPTURE

CONTINUOUS LIFT UP

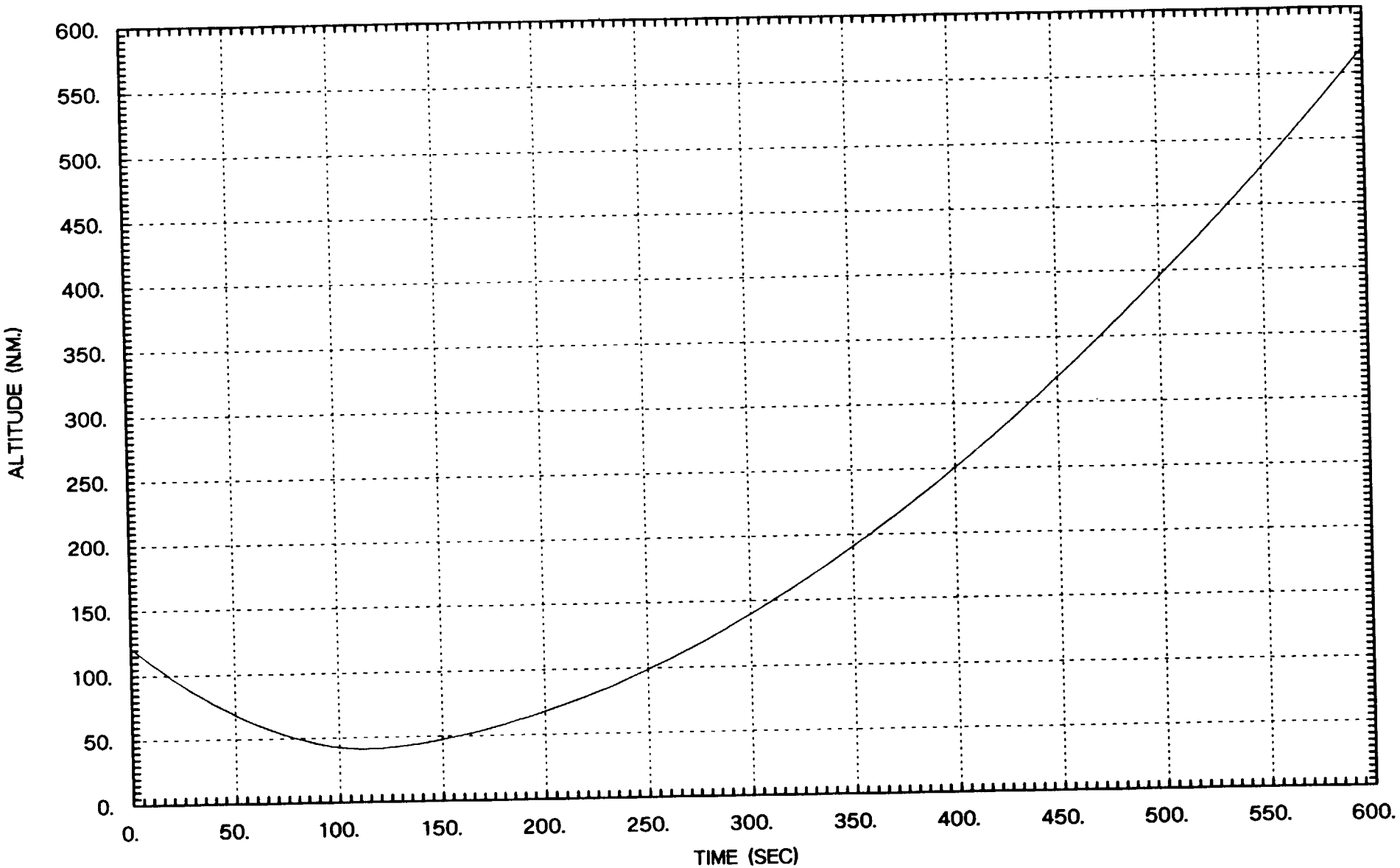
600.
550.
500.
450.
400.
350.
300.
250.
200.
150.
100.
50.
0.
ALTITUDE (N.M.)
0.
50.
100.
150.
200.
250.
300.
350.
400.
450.
500.
550.
600.
TIME (SEC)

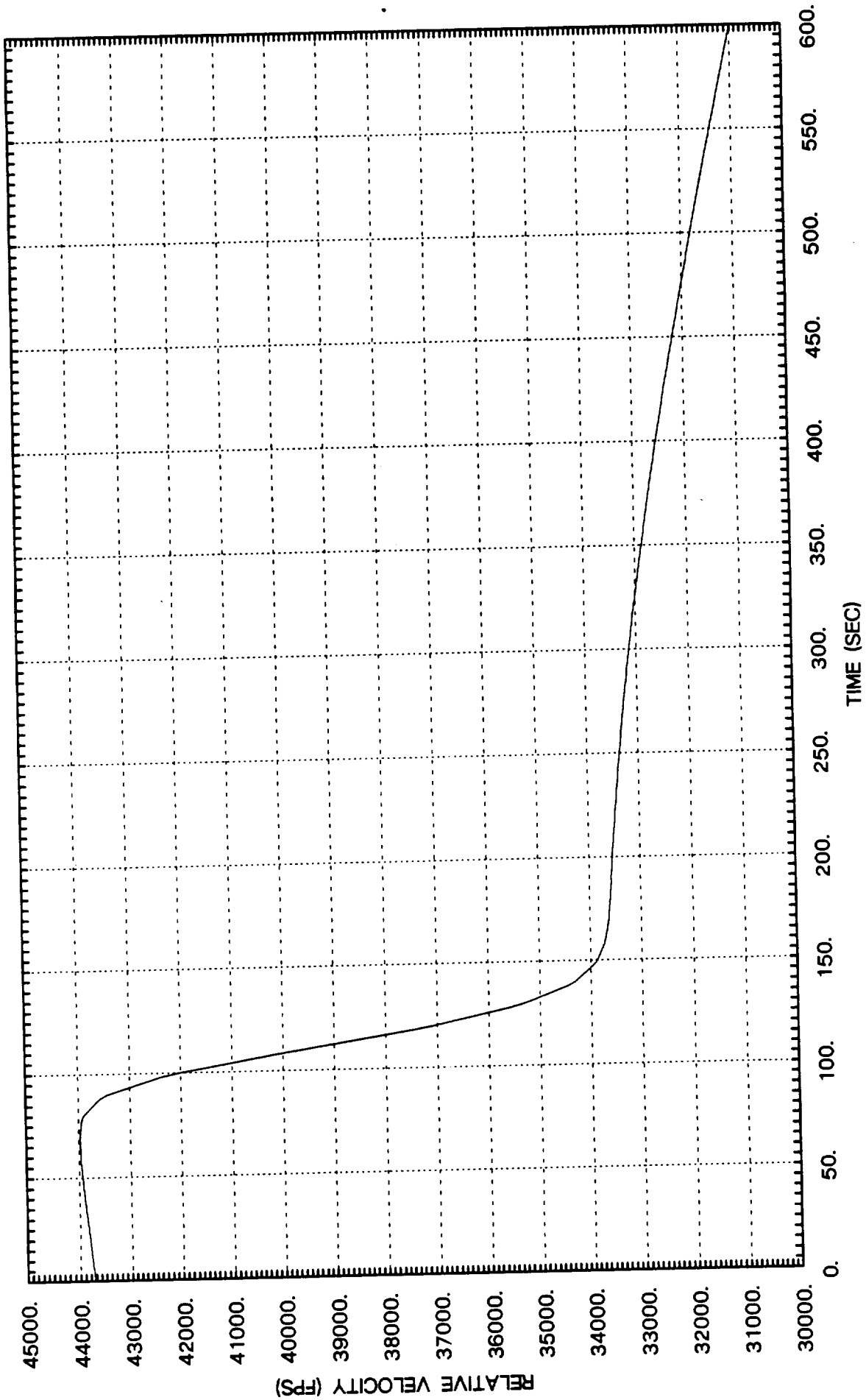
RELATIVE VELOCITY (FPS)
45000.
44000.
43000.
42000.
41000.
40000.
39000.
38000.
37000.
36000.
35000.
34000.
33000.
32000.
31000.
30000.
0.
50.
100.
150.
200.
250.
300.
350.
400.
450.
500.
550.
600.
TIME (SEC)

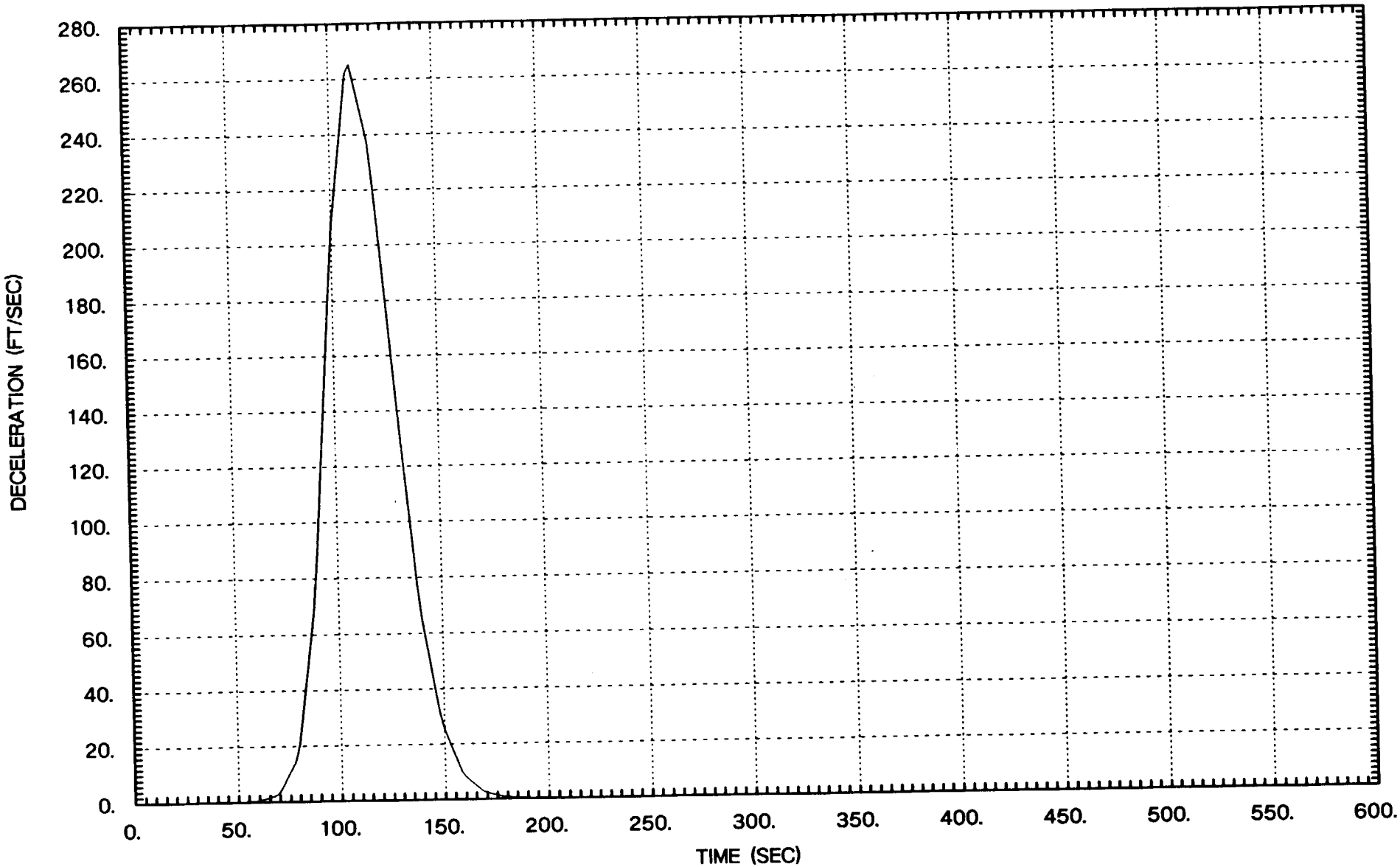
DECELERATION (FT/SEC)
280.
260.
240.
220.
200.
180.
160.
140.
120.
100.
80.
60.
40.
20.
0.
0.
50.
100.
150.
200.
250.
300.
350.
400.
450.
500.
550.
600.
TIME (SEC)

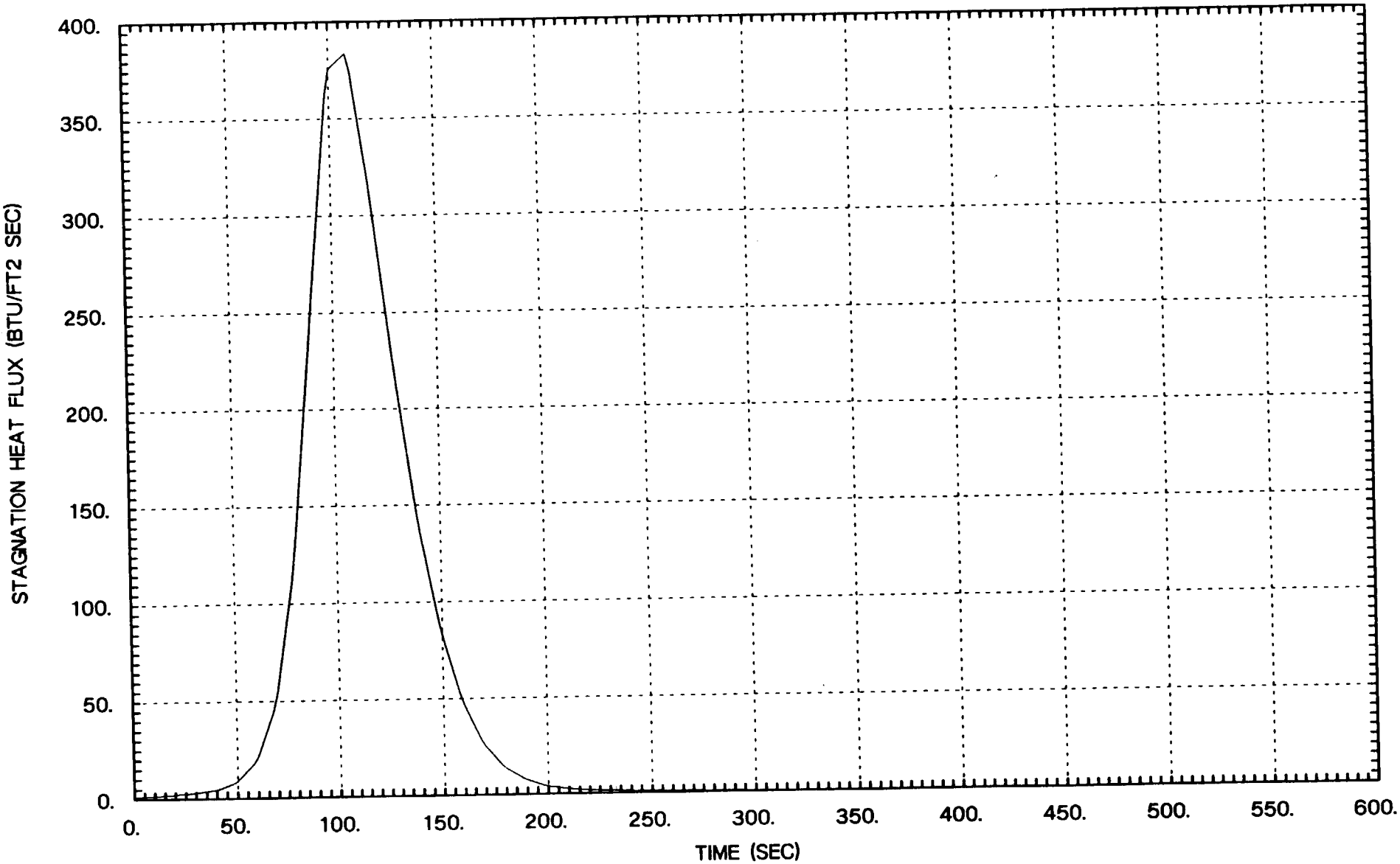
STAGNATION HEAT FLUX (BTU/FT2 SEC)
400.
350.
300.
250.
200.
150.
100.
50.
0.
0.
50.
100.
150.
200.
250.
300.
350.
400.
450.
500.
550.
600.
TIME (SEC)

APPENDIX F

OPEN-LOOP AEROPASS SIMULATION

EARTH CAPTURE

CONTINUOUS LIFT DOWN

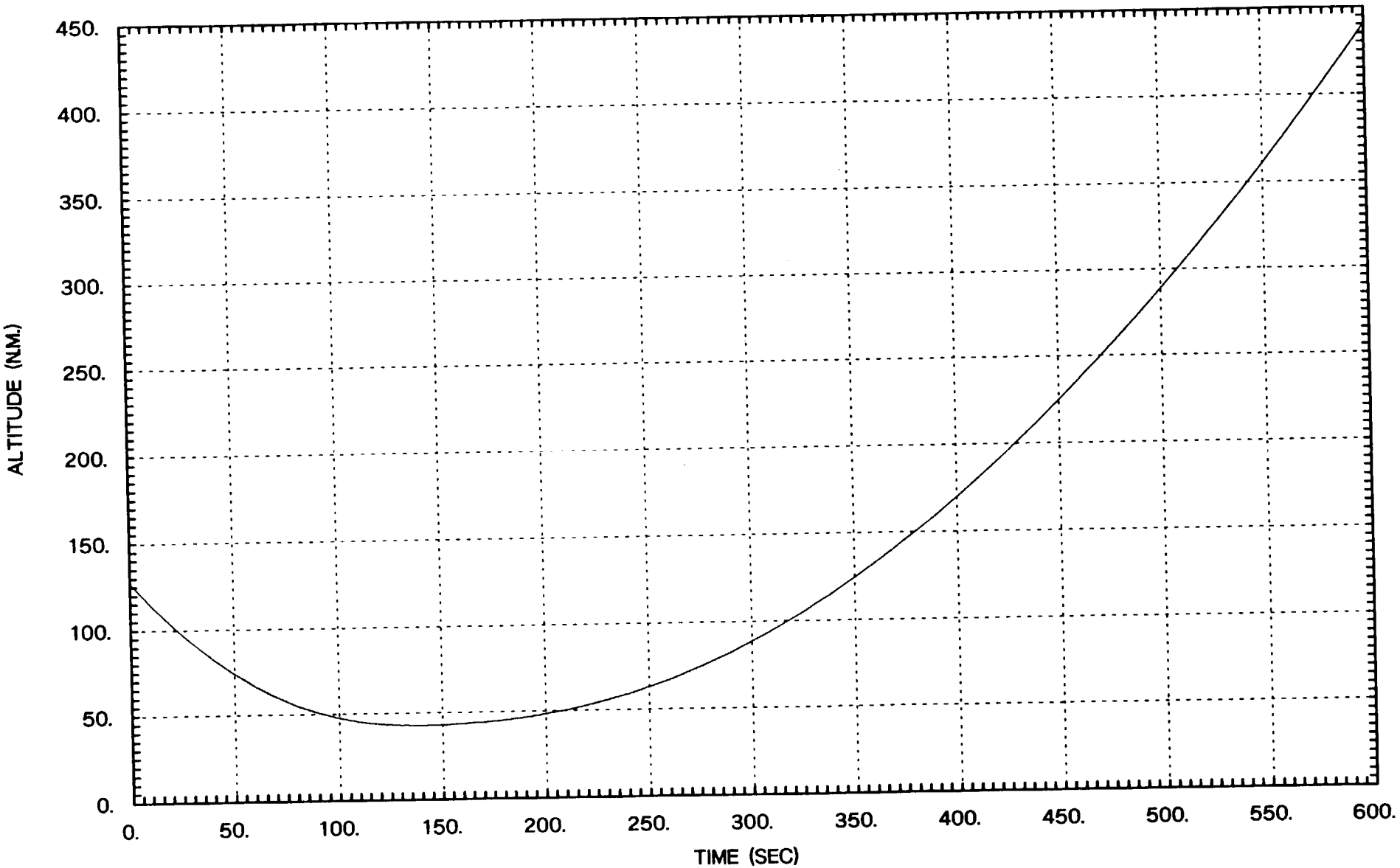
ALTITUDE (N.M.)
450.
400.
350.
300.
250.
200.
150.
100.
50.
0.
0.
50.
100.
150.
200.
250.
300.
350.
400.
450.
500.
550.
600.
TIME (SEC)

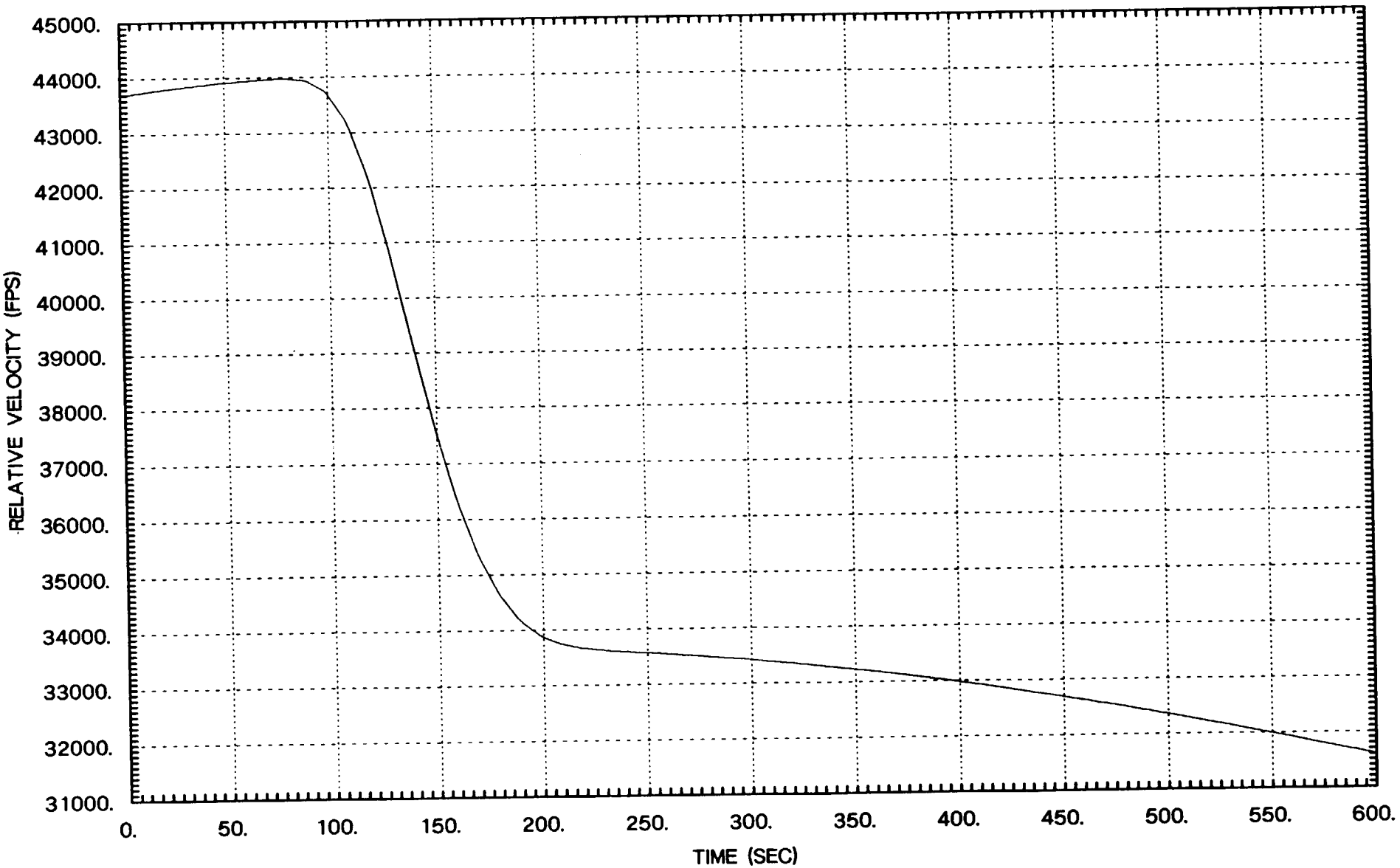
45000.
44000.
43000.
42000.
41000.
40000.
39000.
38000.
37000.
36000.
35000.
34000.
33000.
32000.
31000.
RELATIVE VELOCITY (FPS)
0.
50.
100.
150.
200.
250.
300.
350.
400.
450.
500.
550.
600.
TIME (SEC)

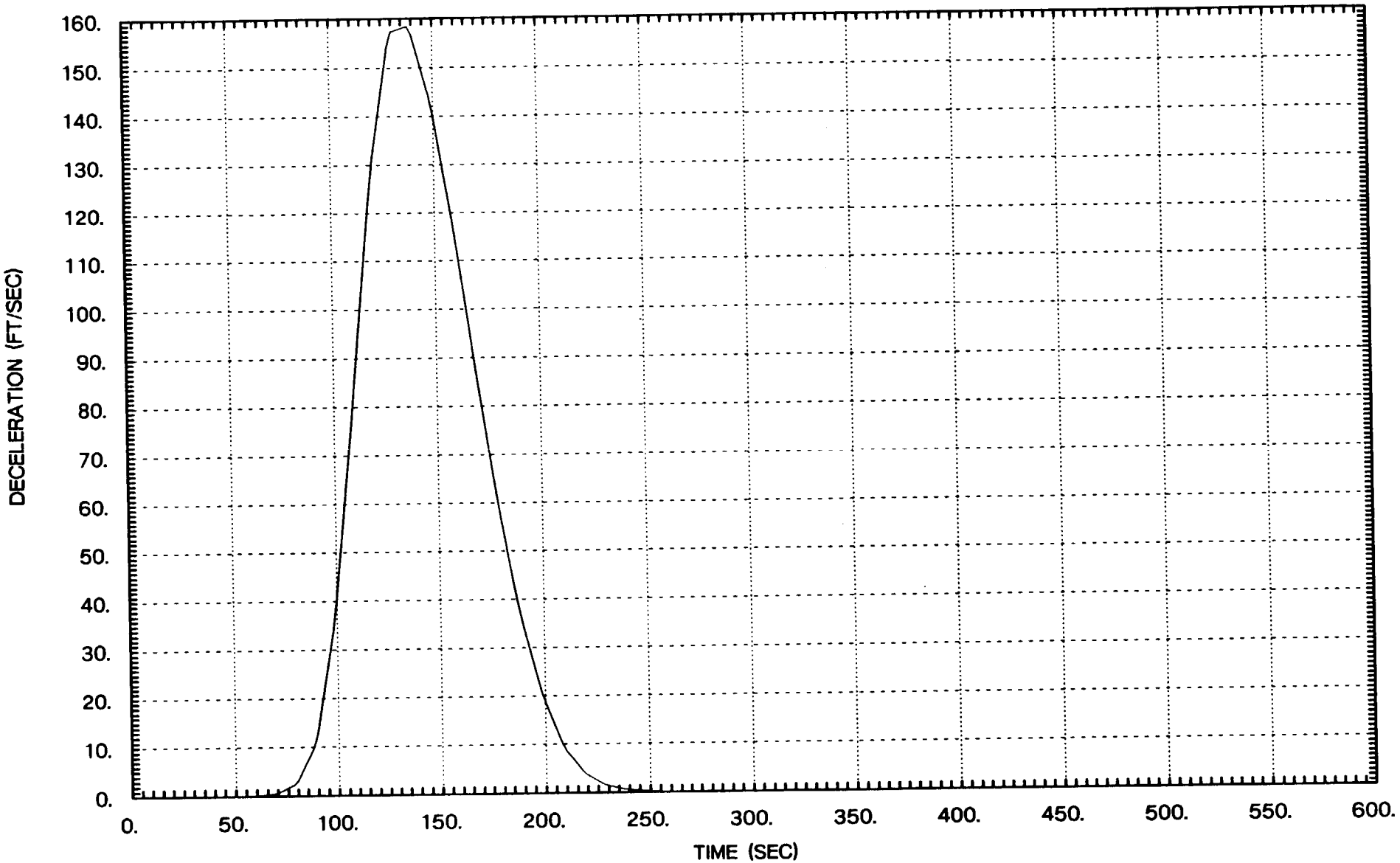
DECELERATION (FT/SEC)
160.
150.
140.
130.
120.
110.
100.
90.
80.
70.
60.
50.
40.
30.
20.
10.
0.
0.
50.
100.
150.
200.
250.
300.
350.
400.
450.
500.
550.
600.
TIME (SEC)

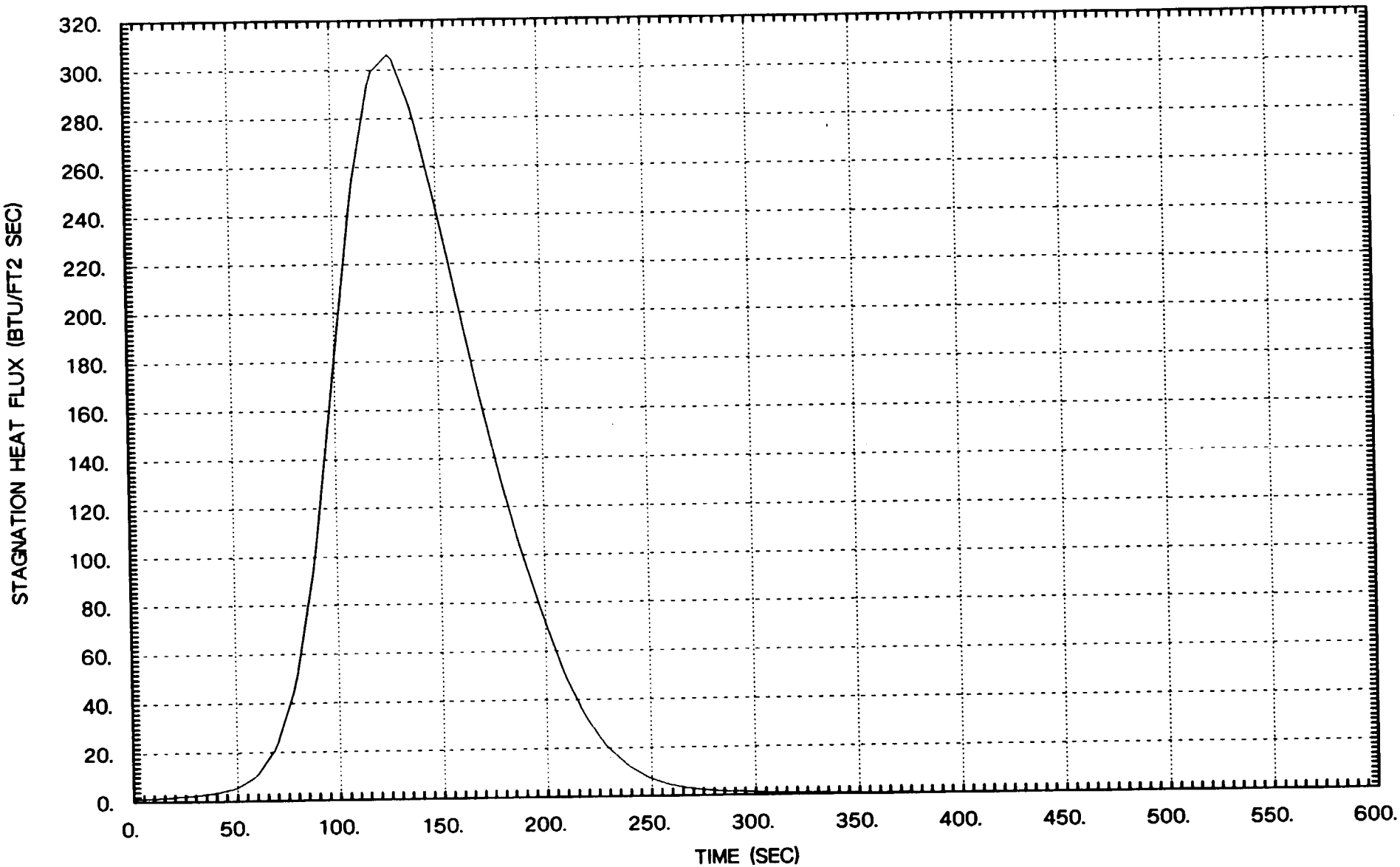
STAGNATION HEAT FLUX (BTU/FT2 SEC)
320.
300.
280.
260.
240.
220.
200.
180.
160.
140.
120.
100.
80.
60.
40.
20.
0.
0.
50.
100.
150.
200.
250.
300.
350.
400.
450.
500.
550.
600.
TIME (SEC)